TAMPERE UNIVERSITY OF TECHNOLOGY

ILARI JÄÄSKELÄINEN

TAIL THREADING ANALYSIS FOR AIRBORNE PULP DRYER

Master of Science Thesis

Examiner: Professor Matti Vilkko
Examiner and topic approved in the Faculty of Automation, Mechanical and Materials Engineering Council meeting on 4 April 2012

TIIVISTELMÄ

TAMPEREEN TEKNILLINEN YLIOPISTO
Automaatiotekniikan koulutusohjelma
ILARI JÄÄSKELÄINEN: Sellun leijukuivaimen päänvientivaiheen analysointi
Diplomityö, 54 sivua
Marraskuu 2012
Pääaine: Prosessiautomaatio
Tarkastaja: prof. Matti Vilkko
Avainsanat:Markovin piilomalli, sellun kuivaus, leijukuivain, päänvienti

Tässä diplomityössä käsitellään sellun kuivausprosessin kuiturainan päänvientivaihetta eräällä Stora Enson tuotantolaitoksella Suomessa. Työssä kehitetään työkaluja, joilla voidaan tutkia vuorojen toimintaa päänvienneissä, selvittää ongelmakohtia ja määrittää päänviennin aikana syntyvien katkojen syitä.

Työn alussa esitellään käytetyt menetelmät. Työssä tutkittiin tehtaan sellunkuivauslaitteistoa ja päänvientiproseduuria haastattelemalla kuivauslaitoksen käyttöhenkilöstöä ja muuta henkilökuntaa. Sellukuivaimen päänvientiproseduuri on hyvin monimutkainen sarja työtehtäviä ja -vaiheita, jotka tulee suorittaa tietyssä järjestyksessä. Seuraavaan työvaiheeseen voidaan siirtyä vasta tiettyjen kriteerien toteutuessa. Päänvientiproseduuriin sovellettiin Markovin piilomallia jakamalla proseduurin vaiheet kahden piilomallin tiloiksi. Piirteet tilojen tunnistamiseksi määritettiin käytyjen haastattelujen perusteella.

Kehitetyt tilamallit sisältävät kuusi tilaa. Työssä luotujen mallien parametrit viritettiin käyttämällä valvottua opetusmenetelmää. Mallit validoitiin vertaamalla prosessitilan videotallenteita mallien määrittämään tilasekvenssiin ja käyttämällä Confusion Matrix -laskentaa opetettujen ja estimoitujen tilojen välillä.

Confusion Matrix -laskennan ja videointien perusteella mallien todettiin toimivan luotettavasti. Määränpään mallin tilamäärittelyissä on suhteellisesti enemmän virheitä, mikä voinee osittain johtua mittausdatan näytteenottotaajuuden pienuudesta suhteessa päänviennin alkuvaiheen työtehtävien lyhyisiin kestoihin. Epätarkkuuksien vaikutusta pyrittiin vähennetämään tilaestimaattien jälkiprosessoinnilla. Kuivanpään mallin tilamäärittelyissä saavutettiin hyvin korkea varmuus (yli 99%). Laskennat suoritettiin Matlab©-ympäristössä.

Määritellyistä tilasekvensseistä laskettiin tunnuslukuja vuoroittain. Tässä työssä tunnuslukuja esitellään osittain yksinkertaistettuina. Tunnuslukuosiossa tutkitaan eri vaiheiden ajallisia kestoja, kärjen syöttöjen määriä päänviennin alussa sekä vuorojen epäonnistuneiden päänvientien katkojakaumia eri tilojen välillä. Tutkinnat on tehty erikseen päänvienneille katkoista ja seisokeista.

Eri vaiheiden ajalliset kestot päänvienneissä katkoista ja seisokeista ovat hyvin samanlaiset, mikä viittaisi vuorojen toimivan päänvienneissä samoin lähtötilan-

teesta riippumatta. Kuitenkin kaikkien vuorojen onnistumisprosentti on huonompi päänvienneissä seisokista. Tämän perusteella vuorojen toimintamallit päänvienneissä katkoista eivät välttämättä sovellu päänvienteihin seisokeista, vaan näitä menetelmiä tulisi kehittää erikseen.

Tutkimuksissa havaittiin, että vuoroilla on vahvuuksia ja heikkouksia päänvientiproseduurin eri vaiheissa. Tekemällä jatkotutkimuksia vuorojen toiminnasta, voitaisiin kenties löytää varmimmat menetelmät kuhunkin vaiheeseen.

Tutkinnan aikana havaittiin myös ongelmia eräässä prosessin mittauksista. Mittauksen perusteella sellurata on korkeammalla kuin tavallisesti ja automaatiojärjestelmä pyrkii laskemaan rataa vähentämällä prosessin nopeuksia. Mittauksen mukaan rataa ei tästä huolimatta saada laskettua. Ongelmat mittauksessa voivat osaltaan vaikuttaa suurestikin päänviennin onnistumiseen. Syitä mittauksen käyttäytymiseen ei tämän työn aikana löydetty.

ABSTRACT

TAMPERE UNIVERSITY OF TECHNOLOGY
Master's Degree Programme in Automation Technology
ILARI JÄÄSKELÄINEN : Tail threading analysis for airborne pulp dryer
Master of Science Thesis, 54 pages
November 2012
Major: Process Automation
Examiner: prof. Matti Vilkko
Keywords: Hidden Markov Model, pulp drying, airborne pulp dryer, threading

In this thesis the tail threading procedure for a pulp drying plant in a Stora Enso's manufacturing plant in Finland is examined. Tools are developed to analyze the work shifts' operation during tail threading, examine the most problematic work stages and to determine causes for web breaks.

The used methods are presented in the beginning of this thesis. The process environment and the threading procedure were studied by interviewing the staff at the plant. The threading procedure is a very complex series of work tasks, which must be completed in order. The next work stage may be started only after certain criteria are fulfilled. Hidden Markov Modelling was applied to the procedure by dividing the tasks as hidden states into two models. The observations used to distinguish the work tasks were developed according to the interviews.

The developed Markov models consist of six state. The model parameters were taught using supervised learning method. The models were validated by comparing video recordings from the process environment with the state sequence estimate given by the model, and also by using Confusion Matrices between the taught and estimated system states.

According to the Confusion Matrix calculations and the video material comparison, the models are found to function reliably. The wet end model's true states are confused with the other states more often than those of the dry end model. This may partly be related to the low sampling rate of the data and the short duration of the wet end work stages. The effects of inaccuracies in state recognition are minimized by post-processing the state estimates. For the dry end model state recognition a very high level of confidence was achieved (over 99%). The calculations for this thesis are done in Matlab©-environment.

Key figures were defined from the state sequence estimates. In this thesis, these characteristics are simplified for presentation. The characteristics include durations in various threading stages, the number of threading efforts and the distribution of web breaks between the different stages for each of the work shifts. These examinations are made for threadings from web break and stoppage separately.

The durations of the examined work stages are very similar for threadings from

web break and stoppage, which could suggest that the shifts use similar threading methods regardless of the situation. However, for all the shifts the success rate is lower when threading from stoppage. This could suggest that the shifts' methods for threadings from web break may not apply to threadings from stoppage, and these methods should be developed separately.

The analysis suggests that each work shift has strengths and weaknesses in different stages of the procedure. By further examining the shifts' operations, the most reliable methods for each work phase could be obtained.

During the research for this thesis some issues with one of the process measurements were discovered. According to the measurement, the pulp web is higher than normal, and the automation system attempts to lower the web by decreasing the speed settings for the process. According to the measurement, however, the web is not lowered. These issues may greatly affect the success of the threading. Cause for this measurement behaviour was not found during the research for this thesis.

FOREWORD

This Master of Science thesis was commissioned by a Stora Enso manufacturing unit in Finland as an individual research project. The supervisor for this thesis was Dr. Tech. Pauli Viljamaa at Vipetec Oy.

Special thanks to the management at the plant for providing me with this fascinating research problem and for all the technical information and support for this thesis and to Esko Similä from Metso Paper for his insight on the process. I would also like to thank the staff at the drying plant for sharing a piece of their enormous expertise and for their support and coffee during the long nights at the plant.

And of course, thank you Pauli and Masa for your support and wise words.

Finally, I want to thank Linda for all the support she has given me during my studies.

Tampere, 21 November 2012

Ilari Jääskeläinen
Insinöörinkatu 59 B 83
33720 Tampere
Tel. +358 44 492 3074

CONTENTS

SYMBOLS AND ABBREVIATIONS

$\boldsymbol{\pi}$	Initial state distribution
$\boldsymbol{\lambda}$	HMM compact notation $\boldsymbol{\lambda} = (\mathbf{A}, \mathbf{B}, \boldsymbol{\pi})$
$\boldsymbol{\lambda}^W$	Wet end HMM
$\boldsymbol{\lambda}^D$	Dry end HMM
φ_t	State tracking array
$\delta_{i,j}$	Kronecker delta, $\delta_{i,j} = \begin{cases} 1, & i = j \\ 0 & i \neq j \end{cases}$
$\mathbf{A}$	State transition probability matrix, $\mathbf{A} = \{a_{ij}\}$
a_{ij}	Probability for transition from state S_i to S_j
$\mathbf{B}$	Emission probabilities, $\mathbf{B} = \{b_j(k)\}$
$\mathbf{CM}$	Confusion Matrix
M	Number of observation symbols
N	Number of HMM states
q_t	State at time instance t
$\mathcal{S}$	Set of possible HMM states
S_i^W	Wet end HMM state i
S_i^D	Dry end HMM state i
t	Discrete time index
t_s	Threading start index
O	Observation sequence $O = o_1, o_2, \ldots, o_T$
$\mathcal{O}$	Observation set $\mathcal{O} = \{v_1, v_2, \ldots, v_M\}$
$P^\star$	Highest state path probability
v_k	Observation symbol, $k = \{1, 2, \ldots, M\}$
$V_t(i)$	Incremental quantity for states $1 \leq i \leq N$, $V_t(i) = \max_{q_1, q_2, \ldots, q_{t-1}} P(\{q_1, q_2, \ldots, q_{t-1}, S_i\} \vert \{o_1, o_2, \ldots, o_t\})$
Q	State sequence $Q = q_1, q_2, \ldots, q_T$
$\hat{Q}$	State sequence estimate
a, b, c, d, e, f	Work shift symbols for shifts 1 to 6 perturbed
HMM	Hidden Markov Model
Threading attempt	Defined by the threading datafile, threading efforts made during the same run of the threading tape
Threading effort	A single effort to accomplish the procedure during the run of the threading tape

1. INTRODUCTION

Stora Enso corporation is one of the world's largest forest industry enterprises. The group employs about 30 000 employees in 35 countries. Their main office is located in Helsinki and the Stora Enso shares are listed on NASDAQ OMX Helsinki (STEAV, STERV) and Stockholm (STE A, STE R). In 2011 Stora Enso's total production capacity is 4.9 million tons of chemical pulp and 11.8 million tons of paper, cardboard and other products. The corporations revenue in 2011 was around 11 billion euros. [4]

Majority of Stora Enso's pulp is manufactured in Finland. Part of the pulp they produce is used in integrated paper and cardboard factories. A large amount of the pulp is dried, baled and packaged to be used at a later time, or to be sold.

The pulp drying process contains several process components [13]. The main components in a drying machine are the headbox, the press section, a steam roll or airborne dryer, a cutting machine and a baling line. The pulp is pumped to the headbox, which spreads the pulp between two felts to form a web. The felts support the web and take it through a series of press rolls at the press section [14]. In a stream roll dryer the web is in contact with steam heated rolls, whereas in a airborne pulp dryer the web is floating on a bed of heated air. In both cases the moisture is removed through evaporation. After excess moisture from the pulp is removed, the web is cut into sheets, which are baled and packaged for storage.

At a pulp drying plant, the production must be halted from time to time. This may be caused by web break during production, or the plant may go to stoppage for maintenance work. Taking the plant back to production efficiently and consistently is economically important. A part of moving the plant back to production from web break or stoppage is to take a narrow strip of pulp through the dryer and incrementally widen the web to full width. This procedure is known as threading.

This thesis was commissioned by a Stora Enso manufacturing unit in Finland. The aim of this thesis is to study the pulp threading procedure for the airborne pulp dryer at the plant and develop tools with which to analyze the procedure automatically. The hypothesis is that each shift has a different approach to the tasks involved in the threading procedure. These differences may result in variation on how well the shifts are able to complete the threading.

In this thesis, a study on the threading procedure at the unit was conducted

in form of interviews with the shift workers and other personnel. Through these interviews, minor differences in the shifts' methods and operation during threading were discovered. The threading procedure itself proved to be a complex set of tasks.

The methods used for this thesis are presented in Chapter 2. The main source of information on the pulp drying environment and threading procedure were the interviews conducted at the drying plant. Process measurement data was data was collected from the plant's database into datafiles containing data for a single threading attempt. To more efficiently analyze the procedure, the tasks in the procedure are defined as process states and modelled using two Hidden Markov Models, or HMM's. In HMM's there is a probability of transition from one state to another. The measurement data is used to define observation symbols, which have a probability distribution between these states [12]. The HMM parameters are taught using supervised learning method, where the correct system output is labeled by the teacher. During training, the output of the model is compared with the desired output and the parameters are adjusted accordingly [8]. Using the acquired model parameters and observation sequence from threading procedure, the most probable state sequence may be solved using Viterbi algorithm [12]. Previously HMM modelling has been used in such fields of study as credit card fraudulent detection [3], mobile machine work cycle recognition [11] and speech recognition [12].

In Chapter 3 the pulp drying environment is presented. Most of the excess water is removed by the time the web arrives at the airborne dryer [5], where the web is taken through several drying levels, supported by a bed of heated air. The heated web is cooled at the bottom of the dryer to prevent brightness reversion and condensation [16]. From the bottom of the dryer, the web is taken to a pull press, which pulls the pulp web through the dryer. Finally, the web is cut at the cutting machine.

The threading procedure, as it is conducted at the drying plant, is presented in Chapter 4. A narrow section of the web, known as the tail, is cut from the web using a water jet cutter. The tail is fed between a threading tape, which takes the tail through the airborne dryer to the pull press. The narrow web is incrementally widened by transposing the web cutter position. At full width the web is taken to the cutter, and as the quality of the pulp is in terms with the mill standards, the baling may begin. At this point, the threading is considered complete, and the plant proceeds to production.

The application of HMM structure to the threading procedure is addressed in Chapter 5. In this thesis the threading procedure is divided between two Hidden Markov Models. In this chapter the model architectures are defined, as well as the measurements and observation symbols required to appropriately distinguish the work tasks. The different characteristics calculated from the state sequences are also introduced.

The models accuracies are discussed in Chapter 6. The threading procedures are examined separately starting from stoppage and web break and the characteristics are discussed. Also, inconsistencies with one of the process measurements were discovered during the HMM analysis which be discussed here.

2. METHODS

In this chapter the different information sources used in this thesis will be discussed. Information on the threading procedure and the process machinery and process control has been mainly acquired through interviews at the drying plant.

2.1 Interviews

The idea of having an interview, is to "collect data through verbal interactions". Interview is an appropriate method of data acquisition for example when the target of the study is a persons visual behaviour. [18]

Depending on how much the chosen questions will control the flow of the interview, the different interviewing methods may be divided into three main categories [18]: structured, semi-structured and unstructured interviews. A structured interview method is commonly used in surveys to ensure the exact same questions for each of the interviewees. A semi-structured interview allows more questions to be brought up as the interview progresses.

2.2 Data acquisition

The different measurement data from the manufacturing plant are stored at the unit's database. For the use of this thesis, a data acquisition scheme has been used to automatically gather data from the database. Data is collected into separate datafiles containing the necessary measurements for HMM analysis.

In this application, the phenomenon of interest is the threading procedure conducted by the personnel at the plant. In order to avoid unnecessary post processing on the data, the datafile's collection will be conducted in such manner, that each datafile contains a single threading attempt.

The different measurement channels and data acquisition will be discussed in more detail in Chapter 4.1.

2.3 Hidden Markov Model

Hidden Markov Model, or HMM, was first introduced in the late 1960's [2], and has been a widely used modelling tool in many fields of study. Such areas of study include

speech recognition [12], credit card fraudulent detection [3] and mobile machines' work cycle [11].

A Hidden Markov Model is a set of states, with each state linked with a probability distribution. The state of the modelled system is transitioned between these states, and the system must be at one of these predefined states at all instances.

Most real-world processes may be observed through different kinds of measurements. These measurements may be discrete or continuous in nature, for example a light is either on or off or the temperature of fluid. The source of the signal may be stationary or non stationary and also corrupted by other signals, for example by noise.

An HMM is characterized by the following [12]. An HMM model may have several hidden state. The number of different states is denoted by N, and the set of these possible states as $\mathcal{S} = \{S_1, S_2, \ldots, S_N\}$. The true state sequence, or the sequence defined by the teacher of the model for time instances $1 \leq t \leq T$, is denoted by $Q = q_1, q_2, \ldots, q_T$. Similarly for the state sequence estimate acquired from the model, let $\hat{Q} = \hat{q}_1, \hat{q}_2, \ldots, \hat{q}_T$.

From the measurement signals distinct observation symbols are defined. Let the number of observation symbols be denoted by M, and the set of observations $\mathcal{O} = \{v_1, v_2, \ldots, v_M\}$ [17]. An observation, also referred to as emission, at time t is to be denoted as o_t. The observation sequence within the time interval $1 \leq t \leq T$ is denoted by $O = \{o_1, o_2, \ldots, o_T\}$ [11].

The emission probability matrix $\mathbf{B} = \{b_i(k)\}$, where $b_i(k) = P(o_t = v_k | q_t = S_i)$, or the probability for observation v_k in state S_i. The rows of $\mathbf{B}$ form the observation probability distribution for each particular state.

Initial state distribution $\boldsymbol{\pi} = \{\pi_i\}$, where $\pi_i = P(q_1 = S_i)$, denotes the probability that the state sequence begins at state S_i

State transition probability matrix $\mathbf{A} = \{a_{ij}\}$ describes the probability of transition from state S_i to another state S_j. Here, $a_{ij} = P(q_{t+1} = S_j | q_t = S_i)$.

The state transition matrix defines the type of the HMM. An HMM is fully connected, if all the elements in A are nonzero. In this case, every state of the model may be reached in a single step from any other state of the model. A fully connected model is also known as an ergodic model. A more restricted model structure compared to the ergodic model is called a left-right model. The left-right model has the property that as time increases, also the state index increases, or alternatively, the index remains [11]. This kind of model structure may be used in processes with clear sequential states.

A cyclic HMM structure is different from the left-right model such that a state

transition from the last state is also allowed to the first state.

Often an HMM is represented in a compact notation $\boldsymbol{\lambda} = (\mathbf{A}, \mathbf{B}, \boldsymbol{\pi})$. In general, the observation sequences may be more than one dimensional and observation probability distributions may be continuous. [17]

Work cycle

A work cycle is defined as a sequence of activities and movements. These tasks are repeated very similarly each time the work is performed. The main objective in work cycle modeling using HMM's is to infer the possibly unobservable intent of the human operator based on observable measurements. In general, the operator of a machine has a certain task or a sequence of tasks that the operator desires to accomplish.

The work cycle recognition with HMM's may be divided into three levels of information [17]. At the lowest level of information are the measurement signals acquired from the examined process. From these measurements observations are extracted. An observation describes features that occur in the measurement data. An example of an observation could be, for example, that signal 1 is below 0 and signal 2 is higher than signal 3. For these occurrences there has been defined an observation symbol on the observation level. Based on the observation symbols, the system's state may be solved for each time instance, denoting the highest level of information. In Figure 2.1 is illustrated an example with three different measurement signals.

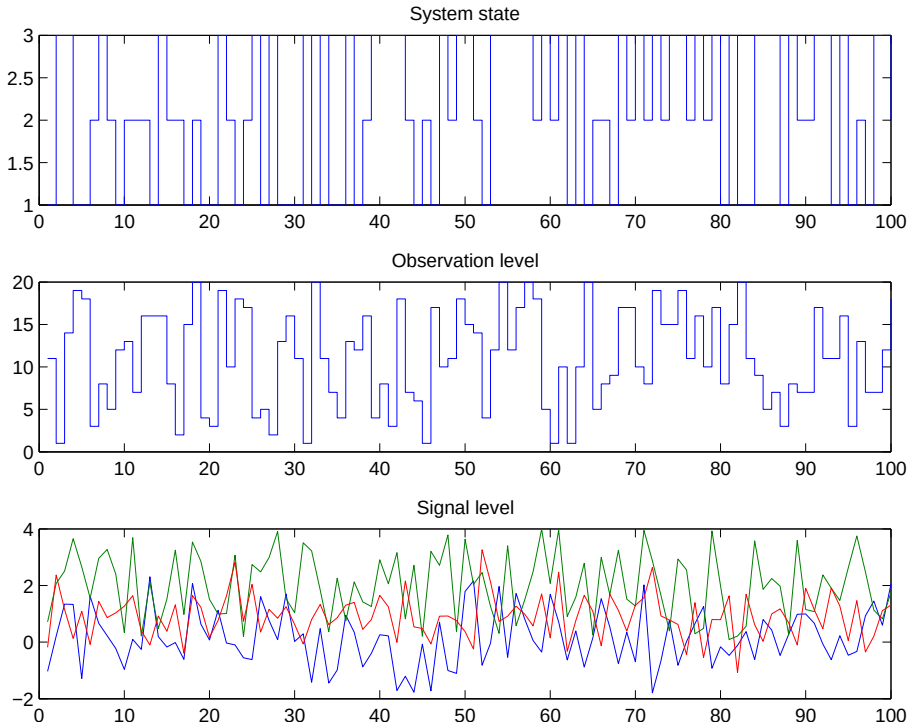

Figure 2.1: Work cycle information levels.

For the example in Figure 2.1, the system has been divided into three states. The state of the system may change at any time instance according to the observations and the model parameters.

A model hierarchy describes how the different states of the system are connected, and how the state may transition. One possible HMM hierarchy for the state transitions shown in Figure 2.1 could be such as shown in Figure 2.2, describing an ergodic model.

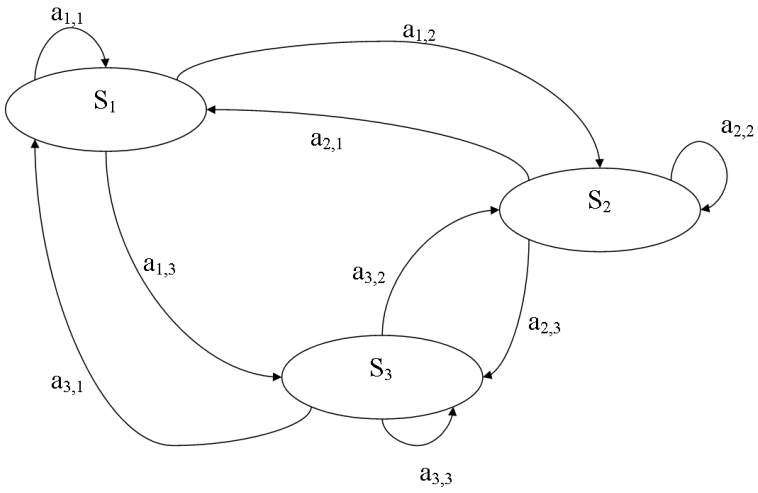

Figure 2.2: A possible HMM hierarchy.

The lowest level of information is obtained from the machine work. At this level the signals may be continuous and affected by noise. Using this measurement data one can extract features, which are used to separate the different tasks in work cycle recognition. The features are basically integer-type events. At the highest level is the system's state at any given time instance. In this example three different measurement signals are taken into account, from which 20 different observation symbols are created.

Using the previous formulation for HMM's there are three basic problems that must be solved in order for the model to be useful in real-world applications [12]

1. Given the observation sequence $O = o_1, o_2, \ldots, o_T$, how to estimate the parameters for $\boldsymbol{\lambda} = (\mathbf{A}, \mathbf{B}, \boldsymbol{\pi})$. This estimation problem is used in training of the model. In case there is labeled training data available, where the hidden states of the system are known, model parameters may be trained using supervised learning.

2. Evaluate the probability of the observation sequence $O = o_1, o_2, \ldots, o_T$ produced by the model $\boldsymbol{\lambda}$. The solution allows the evaluation of how well the model matches the observation sequence. This evaluation problem may be solved using forward-backward procedure [11].

3. How to decode the most likely state sequence $\hat{Q}$ that maximizes the probability of the observation sequence O with given model $\boldsymbol{\lambda}$. In this decoding problem, the most likely path of system states is calculated, taking to account

the sequence of observations O. A recursive method of solving the decoding problem is to use the Viterbi algorithm.

Problem 1 states the evaluation problem, where given a model and a sequence of observations, how to compute the probability for the observed sequence to be produced by the model.

Model parameter estimation

The parameter estimation problem for the work cycle modeling may be performed using either supervised or unsupervised learning. The choice depends on the measurements that are available.

In supervised, or active learning method, the training of the model parameters is done through examples. A teacher, who knows the functionality of the system, provides the input and output of the system [8]. In the case of HMM's, this means to manually define the state of the system at each time instance with the given inputs. This procedure is also known as labeling. After the learning data are labeled, the parameters for the model $\boldsymbol{\lambda}$ may be obtained using simple relative frequency-based probability estimators [17]. As the model parameters are trained, the output result is constantly being compared with the output defined by the teacher [8]. The true state of the system for this method may be obtained using for example video recordings or other additional measurements. It is also essential to select such data for the learning set so that all the possible work cycle scenarios are covered.

Using unsupervised learning method, the training data does not need to be labeled, as opposed to supervised learning [17]. This method relies on good initial guesses for each of the model parameters in $\boldsymbol{\lambda}$. The initial guesses for the model $\boldsymbol{\lambda}$ also determines the hierarchy of the different tasks. This also includes the setting of unwanted transitions to be set to zero in $\mathbf{A}$. In case the initial guesses are made poorly, the model parameters may converge to define a model which does not result in the desired state definitions. [17]

Work cycle decoding problem

As the model $\boldsymbol{\lambda}$ has been trained by either supervised or unsupervised learning, the work cycle recognition involves finding the most likely task sequence given the sequence of observations O and the model $\boldsymbol{\lambda}$. One of the most frequently used for the decoding problem is the Viterbi algorithm. The Viterbi algorithm makes the following assumptions [11]

- The system is at any time t is in one of the finite number of system states

- The observations O and hidden states must be in two aligned sequences of same length. Also, each observation symbol within the observation sequence corresponds to exactly one hidden state.
- The most likely hidden state sequence up to a certain point t only depends on the observation o_t and the most likely state sequence up to q_{t-1}
- At least one path to a state is the most likely one, although multiple state sequences may lead to that given state. This most likely path is selected by the Viterbi algorithm.

These assumptions make it possible to recursively compute the most likely sequence of hidden states given a sequence of observations for a model $\boldsymbol{\lambda}$. To find the most likely sequence, an incremental quantity $V_t(i)$ must be defined for states $1 \leq i \leq N$ [11]

$$V_t(i) = \max_{q_1, q_2, \ldots, q_{t-1}} P(\{q_1, q_2, \ldots, q_{t-1}, S_i\} | \{o_1, o_2, \ldots, o_t\}) \tag{2.1}$$

Therefore, quantity $V_t(i)$ defines the highest probability along a single path, which takes into account the first t observations and ends in state S_i at time t. The probability is maximized using induction [11]

$$V_{t+1}(j) = \max_i (V_t(i) a_{i,j}) b_j(k),\ o_{t+1} = v_k \tag{2.2}$$

In order to retrieve the actual state sequence, it is necessary to take into account the sequence of the states, which maximizes (2.2). Therefore, a tracking array, or a back pointer $\varphi_t(j)$ is defined. This array keeps track of the most likely state transitions.

The actual Viterbi has four steps [11]

1. Initialization
2. Recursion
3. Termination
4. Backtracking of state sequence

At the initialization step, the values for the quantity described in (2.1) and the back tracking array are set for states $1 \leq j \leq N$ [11]:

$$V_1(j) = b_j(k) \pi_j,\ o_1 = v_k \tag{2.3}$$

$$\varphi_1(j) = 0 \tag{2.4}$$

After this, the values are updated recursively using the observations $o_2, o_3, \ldots, o_t$, and maximizing the probability of the state transitions from state $1 \leq i \leq N$ to state $1 \leq j \leq N$

$$V_t(j) = \max_{1 \leq i \leq N} (V_{t-1}(i) a_{i,j}) b_j(k),\ o_t = v_k \tag{2.5}$$

$$\varphi_t(j) = \arg \max_{1 \leq i \leq N} (V_{t-1}(i) a_{i,j}) \tag{2.6}$$

Only the most probable state sequence is taken into account, and all the other paths are discarded.

In the termination step the highest probability for a single path is obtained by

$$P^\star = \max_{1 \leq i \leq N} (V_T(i)) \tag{2.7}$$

where

$$i = \arg \max_{1 \leq i \leq N} (V_T(i)) \tag{2.8}$$

Now the final state $q_t^\star = S_j$. Finally, the most likely state sequence may be found using the back tracking array φ at time instants $t = T-1, T-2, \ldots, 1$ [11]

Logarithmic Viterbi algorithm

If we are to use large pieces of data over a long period of time, the Viterbi algorithm described previously may come to numerical difficulties calculating (2.5). This may be avoided, if logarithms of the model parameters $(\mathbf{A}, \mathbf{B}, \boldsymbol{\pi})$ are used.

Confusion Matrix

To determine how well the HMM is able to explain the behaviour of the modelled phenomenon, we must see how the states calculated by the algorithm corresponds to the set of training data. One method would be to take into account all of the defined system states in a single calculation to have an approximation for the model's capability. This method defines, how many percent the model defines the system's true state in relation to time

$$P = \arg \max_{1 \leq i \leq N} (V_T(i)) \tag{2.9}$$

This method, however, will not provide us with any new information on how well specific states are modelled. Therefore, it would be more practical to calculate how well the model gives the specific states correctly, and possibly, how often the model gives the wrong state and with which state the true system state is confused with.

In order to compare the systems true states with those estimated through Viterbi algorithm, let the true state sequence be denoted by $Q = q_1, q_2, \ldots, q_T$, and the estimated state sequence by $\hat{Q} = \hat{q}_1, \hat{q}_2, \ldots, \hat{q}_T$. The Kronecker delta is a function of two variables, and is defined as

$$\delta_{i,j} = \begin{cases} 1, & i = j \\ 0 & i \neq j \end{cases} \tag{2.10}$$

On many occasions the most interesting quantity could be the amount of time classified correctly or incorrectly. Let τ denote real world time at time instance t. The Confusion Matrix with respect to time is defined as [17]

$$CM_{i,j}^{time} = 100\% \frac{\sum_{t=2}^{T} (\tau(t) - \tau(t-1)) \delta_{q_t,i} \delta_{\hat{q}_t,j}}{\sum_{t=2}^{T} (\tau(t) - \tau(t-1)) \delta_{q_t,i}} \tag{2.11}$$

On some cases, the amount of time classified correctly may be irrelevant. For example in the case with data using uniform sample time, (2.11) may be presented as [17]

$$CM_{i,j}^{events} = 100\% \frac{\sum_{t=1}^{T} \delta_{q_t,i} \delta_{\hat{q}_t,j}}{\sum_{t=1}^{T} \delta_{q_t,i}} \tag{2.12}$$

In the case of perfect classification, both (2.11) and (2.12) would result in an identity matrix.

3. PULP DRYING PROCESS

The pulp and paper industry produce paper, pulp, board and other products using different types of wood as raw material. The industry also produces by-products such as turpentine and tall oil. [7]

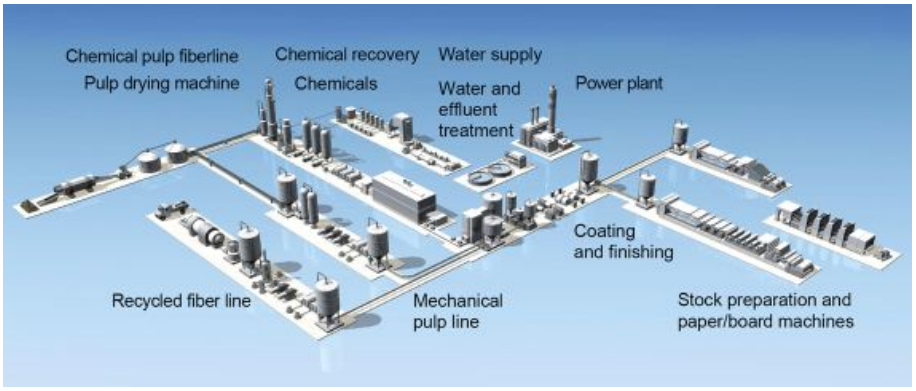

Figure 3.1: Main processes [15].

The main processes in a common forest industry mill are presented in figure 3.1.The wood fibers are separated at the fiber line using mechanical or chemical pulping methods. A supply of mechanically debarked wood is cut into chips or smaller logs and stored for use. In forest industry several wood species are used for different purposes and each have different properties. There are several methods of separating the wood fibers.

Using mechanical pulping the fibres are separated using grindstones, or alternatively refiner plates. The manufactured pulp is called mechanical pulp or refiner mechanical pulp, respectively. The wooden chips may also be steamed prior to grinding, in which case the product is called thermomechanical pulp, or TMP. Other mechanical pulp include grindwood pulp, pressure grindwood pulp and chemithermomechanical pulp. [16]

In chemical pulping the method of separating the wood fibres is based on removing the chemical binding the fibres together, known as lignin. Currently the dominant chemical pulping process is known as alkaline kraft pulping. The process is energy efficient, and high recovery of cooking chemicals reduce pollution [5]. A drawback of chemical pulping is that some of the wood fibres are dissolved during the cooking process. Depending on the wood species and used process, the pulp yield is about

60% with 10% lignin content. [6]

All of these methods require the wood fibres to be immersed in water. In chemical pulping the final step in the process is post screening, after which the pulp is taken to the pulp drying machine. This post screening is operated at 3% consistency [5].

3.1 Pulp drying

All manufactured pulp is not immediately used at the plant to make a final product, but the pulp may be stored or sold. In order to store and transport pulp, the excess water must be removed from it. Excess moisture in the pulp may result in loss of the product due to rotting or mildew [13]. Also, excess moisture is an unneeded transporting expense. Usually the target moisture content of the final dried pulp is 10 to 5% [14]. If the pulp is dryer than this, it will more easily rehydrate from air moisture.

Pulp is dried in a series of processes designed to remove water from the pulp. At each section of the process different methods are used in order to increase the pulp's dry solids content. The most common drying machine sections are the headbox, wire section, press section, and the drying section. The drying section may be a cylinder dryer, where the pulp web is taken through series of steam-heated rolls, or a more modern airborne dryer. [13]. Of all the water or moisture removed from the pulp, 94% is removed at the wire section, 5% at the press section and the last 1% at the drying section [5].

3.1.1 Headbox

Depending on the current production, the appropriate amount wood fibre is pumped to a mixing tank at the drying plant. The fibres are mixed with chemicals and fillers according to the producer's recipe. Previously dried pulp may also be included to this mixture. If pulp is added, it must first be pulped, after which it is taken to the mixing chest. Pulping is discussed later in this chapter.

The dry content of the pulp at the mixing chest is relatively high, and must be further diluted. This pulp is stored at the machine chest at about 4% dry solids content.

The pulp is pumped to the drying machine's headbox. The function of the headbox is to uniformly spread the pulp onto the wire [5]. The pressure inside the headbox is maintained at desired level so that a jet of pulp is formed from the opening of the headbox.

The pulp jet spreads between two wires, an upper and lower wire. The speed of these wires defines the machine speed for the drying process.

At the wire section, majority of the water in the pulp is removed. This is done by taking the web through a narrowing gap and applying suction beneath the wire.

3.1.2 Press section

At the press section force is applied across the pulp wire by rotary presses. The pressure between the upper and lower press section rolls is maintained by steam. The steam also heats the web as it passes between the presses. At the drying plant, there are three separate presses, each with two felts supporting the web. The felts convey the pulp web between the presses on top and bottom of the web. Between each press, the web is released from the felts and taken to the next press.

3.1.3 Airborne pulp dryer

In an airborne pulp dryer the moisture from the pulp web is extracted by applying a heated air flow to the web. The airstream is applied to both the top and bottom of the web. As the pulp travels through the dryer the airflow also supports the web, making it float on bed of heated air [5]. Usually, the web is fed into the dryer from the top section and taken downwards by turn rolls at both ends of the dryer. This structure creates multiple drying levels inside the dryer. At each level, more water is extracted and the moisture content of the pulp is lowered.

The generic structure of an airborne pulp dryer is illustrated in figure 3.2.

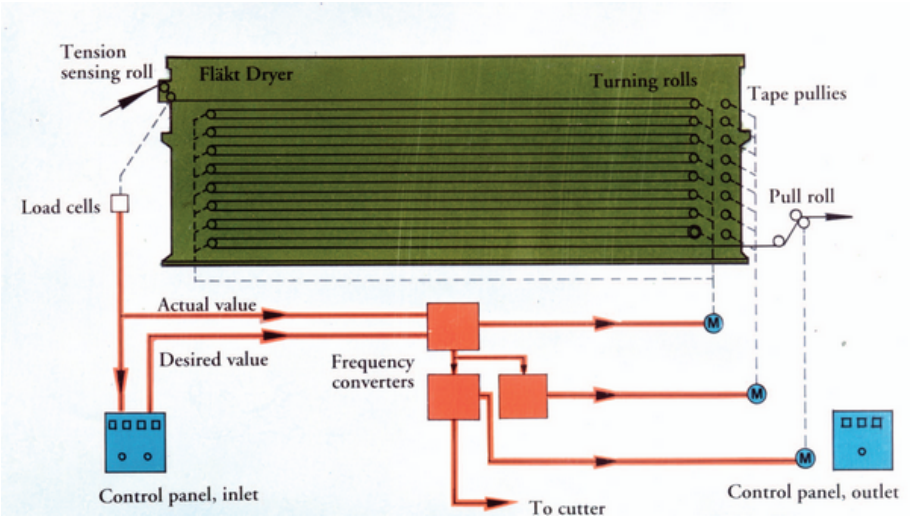

Figure 3.2: Fläkt airborne pulp dryer [1].

The last roll of the press section is located to the left in figure 3.2. The pulp wire is taken from turning roll to the next, between which the wire is supported by a bed of hot air. As opposed to the use of steam-heated rolls, in this method no hot surfaces come in touch with the wire, which in turn helps maintain the quality of the end product.

The air used to dry the pulp is taken from the process environment, and heated using heat exchangers. The air is taken from the bottom part of from the pulp dryer and taken through a heat exchanger, where the air is heated using steam coils. The heated air enters an axial fan, which distributes the air to a set of blow boxes. The air is then distributed to the sheet through nozzles, supporting the pulp between the blow boxes. The heated air moves upwards, and humidity of the air increases as it circulates within the dryer and the heat exchangers. Finally, the humid air is taken from the upper levels of the dryer. The principle of the airblower and heat exchanger are presented in Figure 3.3.

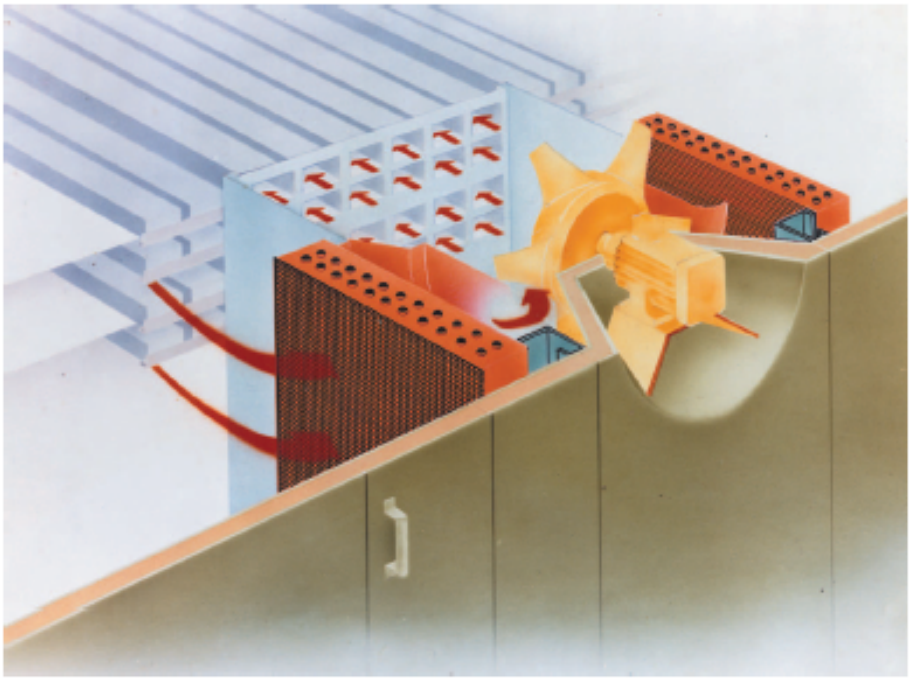

Figure 3.3: Fläkt airblower and heat exchanger [1].

A more detailed view of the blow boxes is illustrated in Figure 3.4.

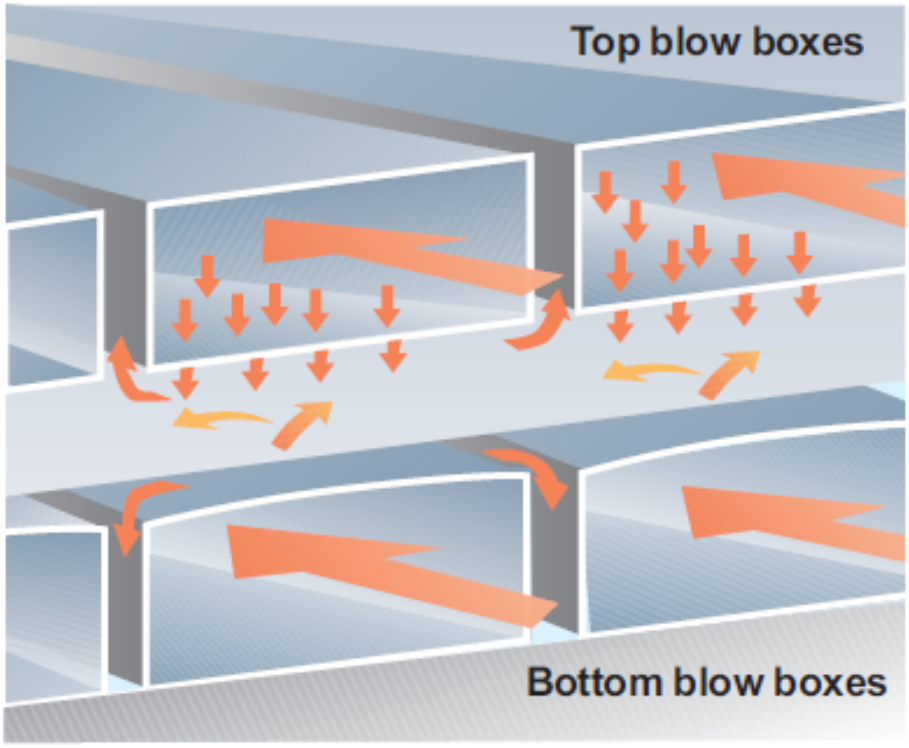

Figure 3.4: Airflow from blow boxes [1].

A more specific outlining of the airborne pulp dryer at the production unit examined in this thesis is presented in Figure 3.5.

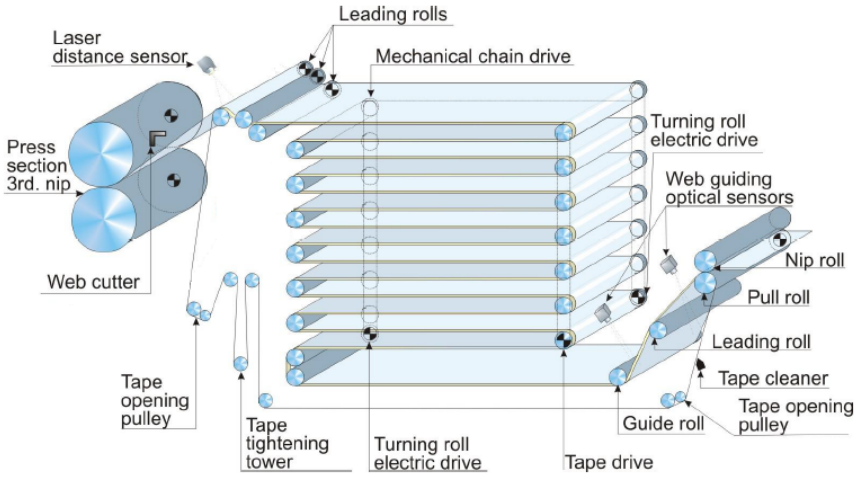

Figure 3.5: Manufacturing unit's airborne pulp dryer [9].

The leading rolls take the web to the upper part of the dryer, from which the web is taken towards the lower part of the dryer from turn roll to the next. The turn rolls located at the press section's side of the dryer are called the wet end turn rolls, and the rolls on the pull roll side the dry end rolls. The lowest turn rolls at both the wet end and the dry end are driven by electric motors. The upper turning rolls are

rotated using mechanical chain drives between the rolls. During production the turn roll electric drives are off, and the pulp web itself turns the rolls. The combination of the pull roll and the nip roll is referred to as pull press.

At the drying plant there are 17 turning rolls on the wet end of the dryer, and 16 on the dry end. This results in 34 drying layers. The lowest layer is the cooling layer, to which the air is blown without heating. The entire cooling layer is independent of the rest of the dryer.

The tension of the web between the press section and the leading rolls is measured using a laser distance sensor. This distance measurement is scaled within the automation system between 0 and 100%. The proper tension is maintained through speed control for the speeds following the press section. The speed setpoint relations are presented in Section 3.2. The tape used to take the narrow pulp strip through the dryer during threading cycles from the leading rolls to the pull press.

Between the airborne pulp dryer and the pull press the position of the web is estimated using optical sensors. Web position control is discussed in Section 3.3.

From the dryer's pull press the web is taken to the cutting machine pull press.

3.1.4 Cutting and baling

The dried and cooled pulp wire is taken to the cutting machine, which cuts the pulp wire in cross direction into same width segments, and also in machine direction into square pulp sheets. As the sheets come through the cutting machine, they are interlaced in machine direction and bundled into stacks. At correct weight, the stacks are taken to the baling line.

At the baling line the pulp stacks are pressed and wrapped in protective paper with production information. The bales are tied with steel wire and finally taken to storage facilities.

3.1.5 Repulpers

A repulper is a machine which is designed to take previously dried pulp added with water and through agitation separate the wood fibres. Rotors within the pulper mix the fibres with water.The resulting pulp is taken to the reject tower, from which this reject may be taken back to the mixing tank.

3.2 Speed control

The pulp drying process consists of several work stages and at each work stage the web is controlled using varying types of turning rolls. As the pulp passes through the different stages at the drying process, the web shrinks and stretches as a result. This is the reason all the rotary devices along the process must be maintained at

slightly different speeds. At the examined drying plant this has been implemented using a setpoint for one speed as a reference for other speeds. The speed setpoints and their relation to each other as implemented at the mill are presented in Figure 3.6.

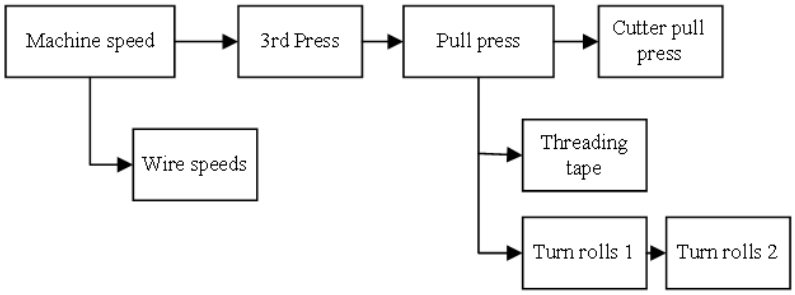

Figure 3.6: Speed setpoint relations.

Figure 3.6 illustrates the dependencies between various setpoints. The setpoint is adjusted by certain percentage for each speed.

3.3 Web position control

Once the threading tape takes the narrow pulp tail to the pulp dryer, the pulp floats on a hot air bed and may move in cross-machine direction. According to the interviews conducted at the plant, the optimal position for the pulp to be positioned in the dryer is about 10 to 20 centimeters from the threading tape.

The position of the pulp may be controlled using three methods: The shift workers have observed that the most straightforward method is to alter the speeds of the axial fans to move the pulp web to desired direction. By altering the fan speeds the position may be controlled according to drying layer. Although ideally, from web position control's point of view, the air from the blow boxes would be released perpendicularly, a study shows the airflow has an angle of departure [10].

Another way to control the movement of the pulp is to apply small changes to the dilution profile. By decreasing the amount of dilution at one end of the web, this side becomes heavier, which results in the web moving towards this end. This method, however, is relatively slow compared to the method of changing the blow from the axial fans.

The position of the pulp web may also be controlled by the guide roll after the pulp dryer's cooling layer. For this method to be effective, the web must be considerably wide, and it may only be used for the lower drying levels of the dryer.

4. THREADING PROCEDURE

The actual threading procedure into the airborne pulp dryer may begin when the pulp web has gone through several steps of drying through the drying presses at the press section.

The basic concept of threading using a single tape threading system is illustrated in figure 4.1.

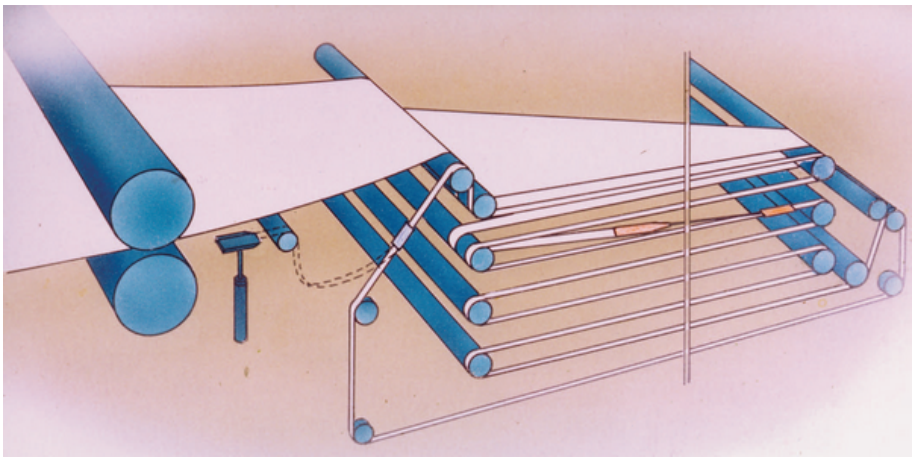

Figure 4.1: The basic concept of threading [1].

As the desired speed for the turn rolls as well as the tape have been achieved, a narrow strip known as the tail is cut from the web from the same side as the tape. The rest of the web is released to the wet end repulper. The narrow feeding-end is cut using a stream of water through a nozzle. The web width entering the airborne pulp dryer is controlled by shifting the cutter in cross-machine direction.

At this point the machine speed dictates the speed at which the web is fed from the last press as described in Chapter 3.

The feeding of the pulp tail into the tape is done by hand, although there are automated feeding systems available commercially. The main challenge is to accurately and safely feed the tail between the threading tape. A common machine speed during web feeding is around 180 m/min, which sets certain requirements for the feeding.

The narrow tail is taken as high as possible, and quickly moved between the opened tape. The tail is fed between the tape for several seconds and then moved to the side.

The slack from the tail taken to the pulp dryer is removed by accelerating the speeds following the third turning press. In this particular production unit this temporary increase in speed setpoint is applied to the cutting machine pull press speed setpoint. The pull press itself does not affect the tail at this time, but the setpoint acts as reference for other speed setpoints as discussed earlier.

Depending on the skill of the person taking the tail between the threading tape, there will be between three to five meters of slack in the pulp web. As the slack is removed, at the same time the pulp web is widened by moving the web cutter incrementally across the web. At this point, the final width of the web will be around 1 meter.

Finally the pulp web is taken high enough for the laser distance sensor to accurately measure the distance of the web. Now the manual increase in the speed setpoints of the turning rolls are removed, and the speeds are determined so that the position of the web measured by the laser is maintained.

The web travels through the airborne pulp dryer at the speed determined by the threading tape. Also, the turn rolls at both ends of the dryer are moving the web towards the end of the dryer. The speed of the turn rolls is set higher than that of the threading tape.

As the web comes through the dryer, it is automatically taken to the cutting machine pull roll. The speed of the turning rolls is incrementally decreased until all the load of pulling the pulp web through the dryer is on the pull press. The turn rolls are provided with overrunning clutches, which make the turn rolls turn at the speed of the pulp web.

The pulp web is widened incrementally after the pulp arrives at the pull press. The rate at which the pulp web may be widened depends on how the pulp behaves in the dryer. According to the interviews, the web tends to shift towards the threading tape as the position of the web cutter is altered..

4.1 Datafiles

Data used for the analysis in this thesis is collected from the manufacturing unit's database. The data is divided into separate datafiles, which include a single threading attempt. The sampling time for the data available in the database is 10 seconds.

In this thesis a threading attempt is defined to begin at the instance the threading tape exceeds a certain speed. This time index is defined as the threading start index, t_s.

The data collection ends in one of four cases: The threading effort ends to the web being at full width, and the recycling hatch is closed, resulting in the plant moving

into production. Data collection for a datafile also ends at the start index of another threading attempt, that is, the threading tape is started again. The plant may also have the need for further maintenance operations, which requires the plant to move into stoppage. In this case, the threading is considered to end as the headbox feed pump is disabled. All of the actions described above may lead to a situation where the data collection for a datafile will not end as early as desired, for example in order to be able to analyze the data. For this reason, the data collection should also be available to be concluded manually.

In order to analyze the beginning state of the process, data is also collected prior to the threading procedure itself. In both the cases of the plant having been in stoppage or the web has broken, three hours of data is collected prior to the start index for each datafile's threading attempt.

This three hour buffer leads to the fact, that the threading tape's speed may exceed the start index threshold several time within one collected datafile. Therefore, in case the datafile does not end in stoppage, the correct start index is determined to be the second to last time the speed rises above the threshold, the last being the starting point for the next file's threading. In case of the plant moving to stoppage, production, or if the collection of data is manually concluded, the start index is defined to be at the point the threshold is exceeded last.

4.2 Examples of threading attempts

In this section some of the basic threading scenarios are presented. As describe earlier, the datafiles are constructed so that the threading attempt begins at the start index t_s. As the data is collected three hours prior the start index at sampling time of 10 seconds, in principle the start index for each datafile is at the index 1081. In practice, however, the start index may vary.

There are five measurements illustrated in the following examples. In the upper subplot the signals are the speed of the threading tape, the position of the web cutter in relation to the threading tape and the speed of the wet end turn rolls. In the lower subplot are illustrated load of the motor on the pull press and the tension of the web between the press section and the dryer (laser distance measurement).

Example 1

In this first example illustrated in Figure 4.2 the threading attempt shortly after the narrow web has been taken to the laser distance measurement. The tail is taken between the threading tape and slack is removed by increasing the speeds in the system. As the slack is removed, the web is at the laser measurement and the tension is maintained automatically at around 75 to 80 % by controlling the speeds within the process. The tension measurement, however falls after a short period of time, indicating that the web has broken either inside the dryer or at the press section. There is a slight increase in the pull press load, indicating that some portion of the tail has come through the dryer. Here it can also be noticed how the speed control tries to compensate the loss in tension by increasing the speeds in the system. The personnel, however, notice the break, and take the web cutter to the far end position.

After some time, the web cutter is taken back to minimum width. The width of the web at this point is approximately 20 cm. Slack is removed, but the workers are not able to remove the slack to take the web to the laser measurement and the web breaks.

Shortly afterwards, the threading tape and the turn rolls are stopped. At the end of the file the turn rolls and threading tape are restarted, indicating the beginning of the next threading attempt.

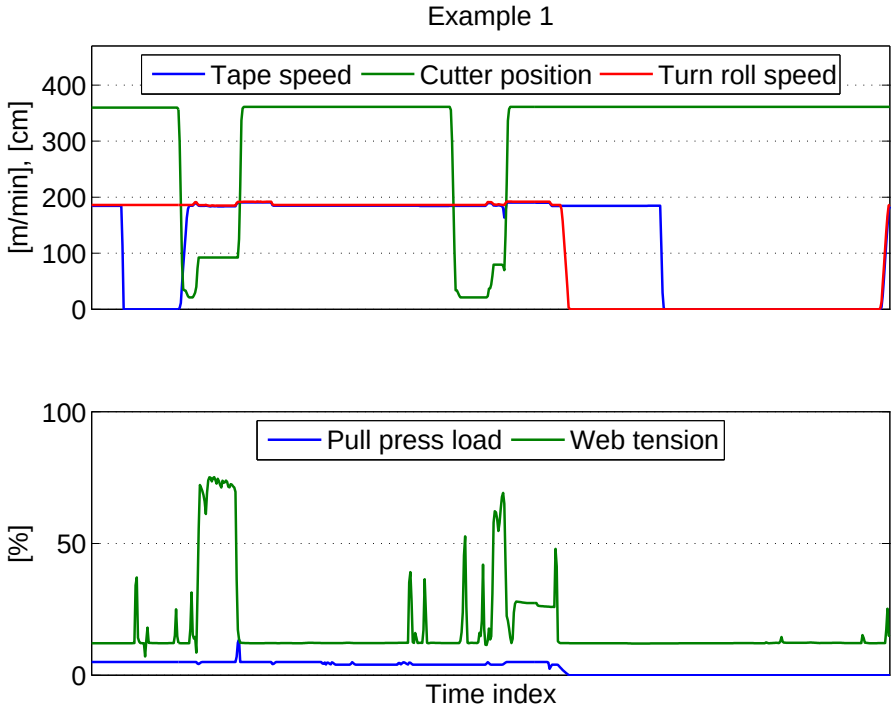

Figure 4.2: Threading attempt example 1.

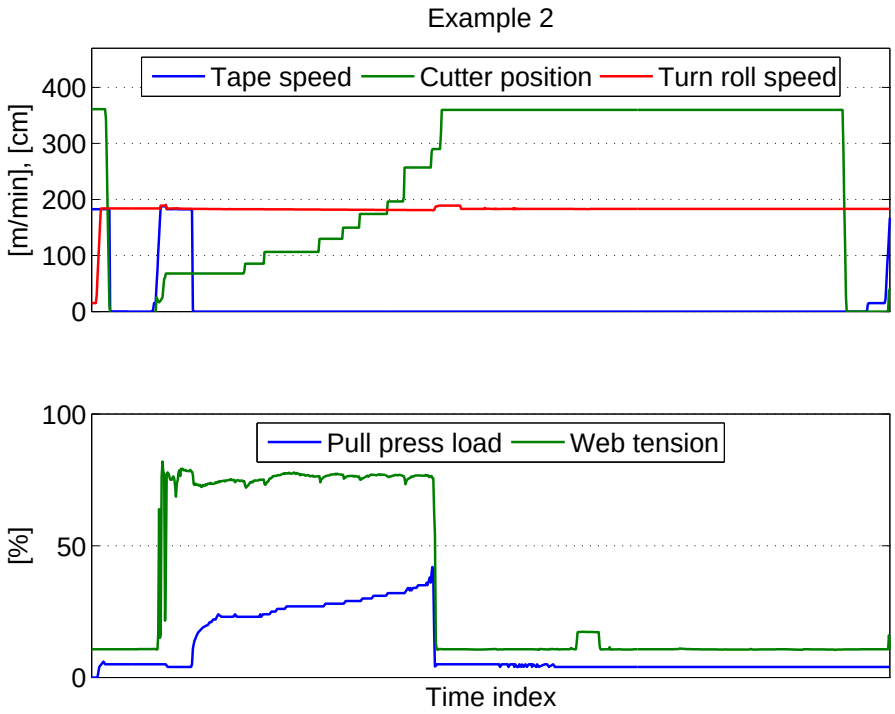

Figure 4.3: Threading attempt example 2.

Example 2

The threading effort illustrated in Figure 4.3 shows an example where the tail is taken through the airborne dryer to the pull press. As the threading begins, the web cutter is positioned at the threading tapes side of the machine. The narrow web is lifted to the laser, as seen by the increase in both speeds. The width of the web is maintained at 70 cm. The threading tape is stopped after the web is taken through the dryer, and the tail arrives at the pull roll. The web causes a sudden increase in the pull roll's motor load.

According to the interviews, the rate at which the pulp web may be widened depends on how the pulp behaves in the dryer. In Figure 4.3 it may be noticed how the width of the web is increased more frequently at some points compared to some instances, where the cutter position is maintained longer. Reason for faster or slower widening of the web may be how the shift is able to control the position of the web, as discussed earlier.

The web is incrementally widened, until the load on the pull roll and the laser distance measurement suddenly drop, indicating a web break. Again, it may be noticed how the turn roll speed is increased as the web tension is lost. At this point, the web cutter is positioned two and a half meters from the threading tape.

The web is taken to full width. As the next threading attempt begins at the end of this datafile, the web cutter is taken back to the threading tape.

Example 3

The third example shows a threading attempt that results in the web being at full width and the plant moving to production. The threading procedure follows the same steps as the previous examples. The position of the web cutter is maintained for longer periods of time at some instances, but finally the web is at full width. It may be noticed how the pull press load decreases sharply near the end of the procedure. At this point the web is taken to the cutting machine's pull press. For a short period of time after this, the recycling hatch taking the pulp sheets to the dry end repulper is closed and the plant proceeds to production.

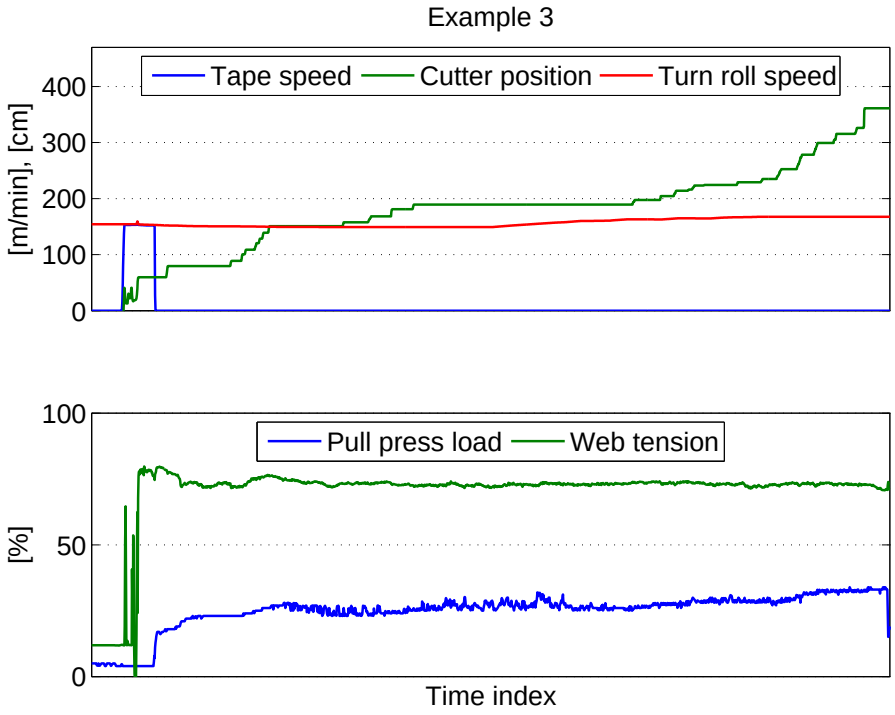

Figure 4.4: Threading attempt example 3.

5. IMPLEMENTATION

A data-acquisition application was implemented to the plant's automation system. The application automatically generates individual data files of all threading efforts. The application monitors two measurements, namely the speed of the tape, and the load of the dryer's pull roll. Under normal circumstances and during production, the tape is not driven but occasionally, to prevent the tape from drying only at one part.

The application creates a new threading file each time the speed of the tape exceeds a certain point, and there is no load at the pull roll, that is, the plant is not currently in production, or there is no previous threading effort under way.

The application also logs three hours before of the triggering instance. This is to visualize the current state of the process and prior events.

There are four different events that trigger the end for logging to the file. The threading effort may end at the following instances

1. the threading is successful and plant moves to production
2. start of a new threading, that is, the tape is stopped and started again
3. the headbox feed pump is stopped, and the plant moves to stoppage
4. the data logging is manually stopped

As the web is at full width and the recycling hatch at the cutting machine is closed, so the cut sheets of dried pulp no longer enter the wet end repulper, the threading procedure is considered finished, and the plant begins production. After this what happens in the process is no longer of interest to the threading procedure, so data logging may be concluded.

In case the threading procedure does not result in closing of the recycling hatch, the threading procedure is considered to have resulted in web break at some point. In case the threading tape at this point has not been stopped, the workers may reattempt the feeding of the tail between the tape. However, if the threading tape has been stopped, as the threading tape's speed once again exceeds the threshold speed, a new datafile for this particular threading attempt is started to log, and the

logging for the previous file is finished.

In case the threading attempt does not succeed, on some occasions the plant must go to stoppage for maintenance. In this case, further threading attempts may not be performed.

In many situations it may prove useful to be able to end the data logging manually. The datafile will normally not be accessible until one of the conditions above is met, but if the data files were to be analyzed as soon as it is obvious that threading will not continue. A situation like this would be, for example, that the threading tape has been stopped, and the web breaks at some point of the procedure.
By the results from interviewing the operators and other staff at the pulp drying plant, the process of bringing the plant to production from stoppage or web break may be divided into separate tasks. These tasks follow a very linear path from the beginning of the threading to the point where the full wide wire is ready to be baled. The tasks in their working order are:

1. Preparing the pulp wire at the final press
2. Cutting the wire to proper width for threading
3. Placing the narrow strip of pulp between the threading tape
4. Removing the pulp strip from the threading tape
5. Removing of slack between the press section and dryer pull press
6. Widening the pulp wire
7. Lifting the wire to the laser
8. Wire goes through the pulp dryer and arrives at the cutting machine pull press
9. Widening the wire incrementally
10. Wire at full width
11. Wire profile adjusted as needed
12. Wire taken to the baling lines cutter
13. Recycling hatch is closed and production begins at baling line

The tasks preceding the wire arriving to the third turning press are not discussed in this thesis.

For the preparing of the pulp, the full width web is taken to the third press and to the wet end repulper. A sample of the web is taken for analysis, and some of the process' variables may be adjusted accordingly. After the variables are adjusted, the pulp wire is slit between the second first and second press-machines using the web cutter. The measurement for the web cutters location is in relation to the edge of the pulp wire. Only this narrow strip is taken to the final press.
The listing of different tasks in their working order strongly suggests that the use of a single HMM model could prove to be rather difficult. As the number of distinct system states increase, so will the number of parameters to be tuned.

Instead of using a single HMM the tasks are divided into two separate models. These models will be referred to as wet end model and dry end model, $\boldsymbol{\lambda}^W = (\mathbf{A}^W, \mathbf{B}^W, \boldsymbol{\pi}^W)$ and $\boldsymbol{\lambda}^D = (\mathbf{A}^D, \mathbf{B}^D, \boldsymbol{\pi}^D)$, respectively.

The wet end model takes into account the tasks from preparing the pulp until the web tail arrives at the baling line's pull press. Respectively, tasks from the arrival of the wire at the baling line until the recycling hatch is closed and the production commences is taken into account in the dry end model.

HMM architecture

The pulp drying procedure is very straightforward and all of the tasks must be completed before advancing to the next task. Also, the procedure may be interrupted at any time, if the wire by any reason breaks. Some of the working tasks discussed earlier, however, are not possible to model due to limitations in measurement signals. Taking these issues into account, the following architectures may be considered for the wet end model in Figure 5.1 and dry end model in Figure 5.2.

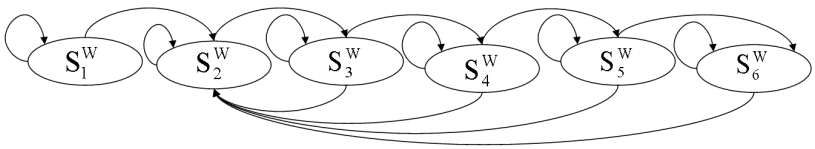

Figure 5.1: Wet end model HMM architecture.

The function and transitions from the wet end model's states are presented in Table 5.1.

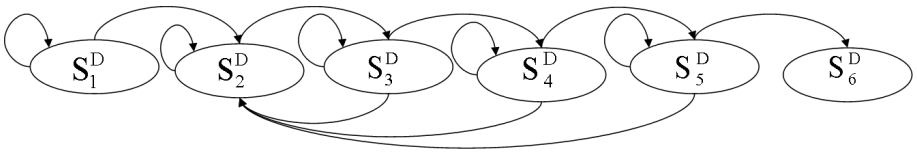

Figure 5.2: Dry end model HMM architecture.

Table 5.1: Wet end model states and transitions

State	Purpose	Transitions
S_1^W	Beginning state, before start index, t_s	To S_2^W at start index, to S_3^W in case web at threading start width at start index
S_2^W	Start index achieved, threading procedure for this attempt begins.	To S_3^W as web at threading start width
S_3^W	Web at threading start width	To state S_4^W as slack removal detected. To S_2^W in case web width no longer at threading width
S_4^W	Slack removal	To state S_5^W as web detected by the laser, to state S_2^W in case of web break
S_5^W	Web detected by laser distance sensor	To state S_6^W as web detected at the pull roll, to state S_2^W in case of web break
S_6^W	Web detected at the pull roll, dry end model state S_3^W	To state S_2^W in case of web break. May occur at dry end or wet end

Similarly, for the dry end model the states are defined as in Table 5.2.

Table 5.2: Dry end model states and transitions

State	Purpose	Transitions
S_1^D	Beginning state, before start index t_s	To S_2^W at start index
S_2^D	Start index achieved, threading procedure begins. System at wet end model's states S_2^W to S_5^W	To S_3^D as web detected at pull roll
S_3^D	Web at pull roll	To state S_4^D as web at full width. To S_2^D in case of web break
S_4^D	Web at full width	To state S_5^D as web taken to cutting machine's pull press, to state S_2^D in case of web break
S_5^D	Web at cutting machine pull press	To state S_6^W as plant is at production, to state S_2^W in case of web break
S_6^D	Plant in production	

For convenience both of the models are defined to begin at state 1, which describes the system state before the start index. Furthermore, the last state of the wet end model corresponds to the dry end model's second state.

Signal level

Based on the interviews performed for the five work shifts, several interesting data signals are discussed, which may be used for modelling the threading procedure.

In order to distinguish the state transitions described in Table 5.1 and Table 5.2, the following signals are taken into consideration as in defining the different observations for the HMM algorithm.

For the wet end model the required signals are

- Position of the web cutter
- Wet end turning roll speed
- Laser distance sensor

- Pull roll load
- Dry end model state

Similarly, for dry end analysis, i.e. after the wire has reached the cutting machine pull press until the procedure reaches production, the signals of interest are

- Pull roll load
- Position of the web cutter
- Recycling hatch state measurement
- Laser distance sensor

Also the start index is used to distinguish the states prior to the threading procedure for both of the models.

Observation level

As discussed earlier, the HMM algorithm is able in some implementations use the data signals directly. In this thesis however, the method of discrete observation symbols are used for both the wet end and dry end models. The observation symbol is defined for every time instance of the datafile, resulting a vector the same length as the datafile. At which order the different symbols are numbered is irrelevant to the functionality of the HMM algorithm.

As designing the different observation symbols for the HMM algorithm, the most important aspect is, obviously, to find such features within the collected process data, so that the defined system states may be distinguished.

Both for the wet end model and the dry end model, the first state may be distinguished by the start index t_s for the particular file. The start index, as described before, is the index of the data, when the speed of the threading tape exceeds a predefined threshold.

For the dry end model, we must be able to distinguish when the tail has come through the airborne dryer and is taken to the pull roll. Although there are no straightforward measurements for the location of the tail, after the different turning rolls in the process have been started, the loads for each roll remains very stable. The arrival of the tail to the pull press may be noticed by the increase of the pull press's motor load, as was also noted in the threading examples in Section 4.2.

The load of the pull press may increase temporarily, namely in the case of multiple threading attempts, where the tail is fed between the threading tape, and for some reason, the web is broken. The tail is taken through the airborne pulp dryer, and

this short piece of pulp may cause the load to increase. This case could be taken into account, for example by examining the tension of the web between the third press and the dryer.

As the threading procedure begins by taking the narrow tail between the threading tape, the width of the web at the third press section nip should be such, that the person feeding the tail may do so safely and definitely. According to the interviews, the web width at which the tail is taken between the tape is between 5 and 20 cm.

For this thesis, a total of 26 observation symbols were developed for the wet end model, and 45 symbols for the dry end model.

Characteristics

According to the interviews, all the shifts have slightly different methods regarding the threading procedure. Although the main tasks discussed earlier must be completed, some methods made to achieve them may prove to be more sufficient than others. For instance, during web widening, some shifts actively attempt to control the movement of the web, as other shifts passively wait for the web to be in a position available for widening.

The key figures calculated from the HMM states for this thesis include

- Number of efforts during single threading
- Time used for each task during the effort
- Number of web breaks from each of the system state

The success or failure for each threading attempt is determined from the final state of the recycling hatch.

Teaching data set

The supervised learning scheme is used for the model parameter estimation problem for this thesis for both the wet end and dry end model. Therefore, for both models there should be a set of threading procedure data files, for which the true state of the system is defined for each time instance. As the signals on the observation level are defined so that they would be able to describe the system's states, the observation vector is calculated for each of the data files in the teaching data set in order to define the true system states more precisely.

As described in the architecture section of this thesis, for both of the models there are certain state transitions that should not occur.

For the teaching data, a set of data files was chosen, so that all the possible state transitions and observation symbols are addressed.

The Confusion matrix acquired through using supervised learning method for the wet end model, as by (2.12) is

$$\mathbf{CM}^W = \begin{bmatrix} 100.0000 & 0 & 0 & 0 & 0 & 0 \\ 0 & 98.6407 & 0.2146 & 1.0016 & 0.1431 & 0 \\ 0 & 1.2097 & 96.7742 & 2.0161 & 0 & 0 \\ 0 & 2.1583 & 0 & 92.0863 & 5.7554 & 0 \\ 0 & 0.1613 & 0 & 0.1613 & 99.6774 & 0 \\ 0 & 0 & 0 & 0 & 0 & 100.0000 \end{bmatrix} \tag{5.1}$$

Similarly, the Confusion Matrix acquired for the dry end model is

$$\mathbf{CM}^D = \begin{bmatrix} 100 & 0 & 0 & 0 & 0 & 0 \\ 0 & 99.9333 & 0.050017 & 0 & 0 & 0.016672 \\ 0 & 0.33944 & 99.6606 & 0 & 0 & 0 \\ 0 & 0 & 0 & 99.9087 & 0.091324 & 0 \\ 0 & 0 & 0 & 0 & 100 & 0 \\ 0 & 0 & 0 & 0 & 0 & 100 \end{bmatrix} \tag{5.2}$$

The models were validated using video recordings from the plant. The state sequence estimates were calculated using the models described in this thesis, and the sequences were compared with the recordings.

6. RESULTS

The results concerning the implementation of the Hidden Markov Models described in chapter 5 will be discussed in this chapter. Also the characteristics and differences between the work shifts will be discussed.

6.1 Model accuracy

Concerning the confusion matrices $\mathbf{CM}^W$ and $\mathbf{CM}^D$ in (5.1) and (5.2), for the wet end model and dry end model, respectively, there is a significant difference between the two models as how well the algorithm gives accurate evaluation for the system states. For both the wet end and dry end model, the state preceding the start index is accurately deducted, according to the teaching data set.

For the wet end model, the next two states are less accurately classified. The state S_2^W is defined to be the state, at which the treading tapes speed is at that of threading, at S_3^W the tail is at feeding width. Still, these classifications are quite satisfactory comparing to S_4^W, at which slack is removed from the web. These problems may be contributed to the sampling rate of the data, being only at $0.1Hz$. Situations at the wet end, however, change quite rapidly, and this results in some difficulty in defining the correct state.

For the dry end models confusion matrix, the classification of states is much more certain. Taken into account the teaching data set, the model states are classified correctly over 99% of the time. Regarding the inaccuracy of evaluating the wet end model's state S_2^W, or the second row of the confusion matrix $\mathbf{CM}^W$ the evaluation reliability could not be improved. However, with further inspection, this uncertainty seems to occur mainly after the tail has arrived at the pull press. If the web breaks after the dry end model's state is higher than S_2^D, that is, the tail has arrived at the pull press, the web break is interpreted correctly by both of the models. After the web break, however, on some occasions the wet end model state sequence and after this goes via S_3^W to S_4^W and back to S_2^W.

This situation could not be resolved in terms of HMM modelling during the research for thesis. However, the negative effects of these occurrences on the calculation of the characteristics is minimized by post-processing of wet end state sequence. This

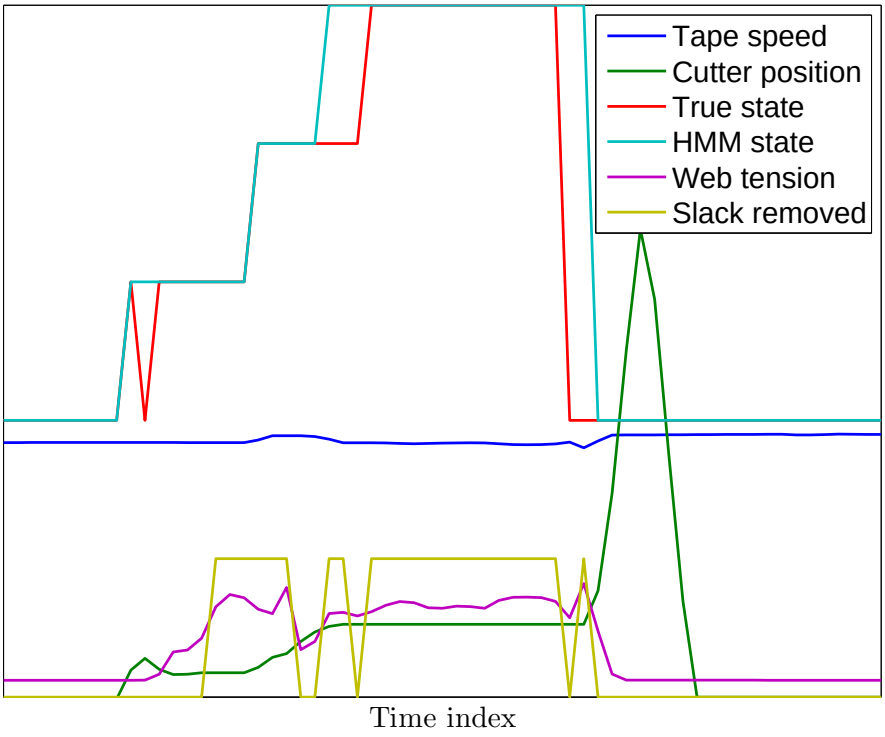

Figure 6.1: Example of laser distance measurement.

was achieved by only taking into account those wet end model states that precede the instance that the tail arrives at the pull press. As the tail arrives at the pull press, the threading tape is stopped, resulting in a new threading attempt in case the threading is unsuccessful.

For the wet end states S_3^W and S_4^W the total number of occurrences in the teaching data set is relatively low compared to the other states. This is due to the position of the web cutter being at feeding width only for a short period of time during the threading. The misinterpreted instances for state S_3^W is limited to two datafiles in the teaching data set. This may be contributed to the sampling rate of the data in relation to the fast execution of these states.

The state S_4^W corresponding to the removal of slack from the web brings difficulties in regards to when the web has been taken to the laser measurement. As the narrow web is being lifted to the laser distance sensor, the web often makes a slight vertical motion. Due to this phenomenon, at one point the narrow web seems to be at the height required for the laser to reliably measure the distance, whereas on the next instance the web may seem too low. An example of this kind of situation is illustrated below in Figure 6.1.

In this illustration, the yellow signal shows when an observation symbol defined

for the wet end model considers that the narrow web has been lifted to the laser measurement. The signals labeled as true state and HMM state denote the true sequence of the wet end states and the state sequence determined by the HMM algorithms, respectively. The state numbers are scaled by 100.

The first difference in the taught state sequence and the state sequence determined by the HMM algorithm, is at the beginning of the threading procedure. The threading tape is already started, but the cutter position shows, that the web is not at feeding width. The web is widened, so that according the observation defined for the wet end model the web is at feeding width for one time instance. The HMM algorithm, however, does not consider the wet end state to transition from threading width back to the previous state in this case.

The first time the narrow web is observed to be at the laser measurement, is due to disturbance in the measurement, for the web has only been at threading width, and no slack has yet been removed. As the slack is removed, the vertical movement of the web causes uncertainty in the determination of when the slack is removed. Here, the HMM algorithm determines the state to transition from S_4^W to S_5^W the first time the web is observed to be at the laser, whereas the teaching of this data considers the transition to occur on the latter observation. Here the HMM's solution may be considered to be more correct, as it may be noticed, that the tape speed has already returned to regular threading speed by the time the teaching considers the state to have changed.

The time index for the occurrence of web break is also slightly different according to the taught states and states determined by the HMM. The real web break is considered to be the instance the web goes too low for the first time. However, the HMM algorithm considers the web to break only the second time the web is not at the laser measurement.

Considering the dry end model's confusion matrix $\mathbf{CM}^D$, the most critical state must be S_2^D, where the tail has not yet arrived at the pull press or the web is broken. In the teaching data set this state is confused with state S_6^D, or the plant proceeding to production. This may lead to incoherence regarding the calculation of the characteristics. The situation seems to occur after the web has been taken to full width and the load on the pull press drops, indicating web break. This is confused with the web being taken to the cutting machines pull press, which also results the load on the pull press to lower. Regarding teaching of this scenario, the situation where the web would break after it was taken to the cutter's pull press has not yet occurred.

One possibility to overcome this problem could have been to remove the state

S_5^D, and have the state transition go straight from full width web to production. However, this could have brought up new problems, due to the fact that web breaks may occur when the web is at full width.

There was no solution found to this situation in term of the HMM architecture or the teaching data set. The problem was resolved by using the definition of the datafiles, and how a data collection is concluded. As the data collection for each datafile may finish only on the occurrence of one of the four situations described in Chapter 5. In this thesis, the system being at state S_6^D is considered to be valid only if the index of this occurrence also denotes the end of the datafile.

6.2 Characteristics

The HMM modelling scheme described in this thesis was used to measure certain interesting aspects regarding the threading procedure. The data available consisted of a considerable amount of tail threading procedures over a certain period of time.

According to the interviews conducted, the threading is different after a regular web break as opposed to the plant having been in stoppage. The possible differences between the work shifts will be looked into, and also the differences of each shift's threading from web break and stoppage.

In the following illustrations, the order of the work shifts has been altered, and the regular numbering is changed to lettering. It should be noted, that for shift b the number of threading attempts is somewhat smaller than that of the other shifts.

The frequencies of the observations in the figures are not presented. The axis for the illustrations are set so that the results from stoppage and web break are comparative.

The machine speed may be different for each threading. At the plant there have been threading attempts with various machine speeds, but mostly the machine speed has been 180 metres per minute. For the duration histograms to be coherent, the analyzed data is limited according to this machine speed.

6.2.1 Threadings from stoppage

In this section, the results for the HMM computation and analysis are presented, as the threading procedure begins with the plant having been in stoppage. The plant is considered not to be in stoppage after the plant has proceeded to production after the headbox feed pump has been stopped.

As described in the definition and functionality of the datafiles, the collection of the previous threading attempt is finished and the collection of the next threading

is triggered at the moment the speed of the threading tape exceeds the threshold value.

In Figure 6.2 is presented the shifts' ability to successfully make the threading and move the plant into production. As the shift may change in the middle of the threading procedure, the data presented here is limited so that the shift that begins the threading also must be the one to finish it, nevertheless the threading is successful or not.

Figure 6.2 shows the percentage of successful threadings for each work shift. Here it may be noticed that there are quite large differences between shifts in terms of how effectively their actions during threading lead to success. For this analysis, the HMM-methods are not used. Here, it is illustrated for the purpose of showing that there are differences between the shifts in terms of effectiveness.

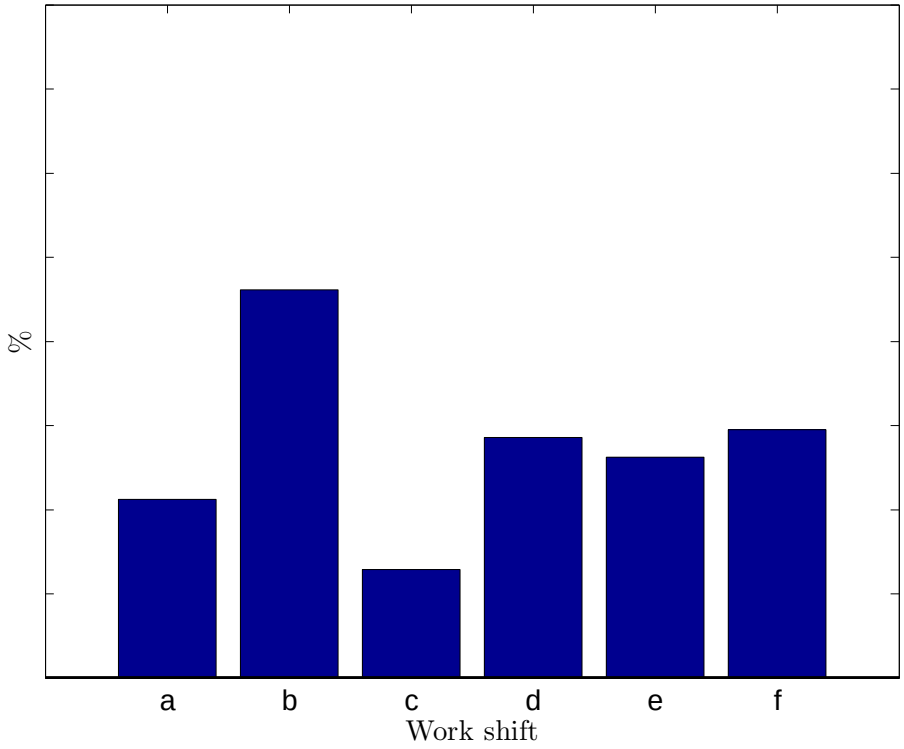

Figure 6.2: Percentage of successful threading attempts in relation to the shift's total number of threadings from stoppage.

Here, shift b seems to most effectively use their available threading attempts to have the plant proceed to production. Shift b success rate is nearly double that of shifts a and d through f, and over three times that of shift c. Obviously, there must be differences between these shifts in terms of how the threading procedure is completed.

Next the duration distributions for the main are process stages are illustrated. The data is limited to the starting and finishing shift being the same, due to the fact

that on shift change the workers will not necessarily immediately actively continue the threading procedure. Also, to the client, the results for this analysis was given according to shifts, whereas in this thesis, the durations are presented generally without comparing the work shifts and the information on the durations and frequencies are not shown.

Due to the fact that if the web breaks during a threading attempt, this may happen at any time at any step of the process. Therefore, in the duration distribution analyses, the data is also limited to successful threadings. Also, as a successful threading attempt may contain several efforts and the system's state may have gone through some of the states and come back to the states denoting start of the threading,

In Figure 6.3 is a histogram presentation of the distribution of time taken from the start index t_s to the tail's arrival at the pull press. Generally speaking, the time it takes for the tail to go through the pulp dryer is the same for threadings with same machine speed from the moment the narrow web is taken out from between the tape. However, in this analysis the differences occur due to work shifts' differences in ability to effectively feed the tail between the threading tape.

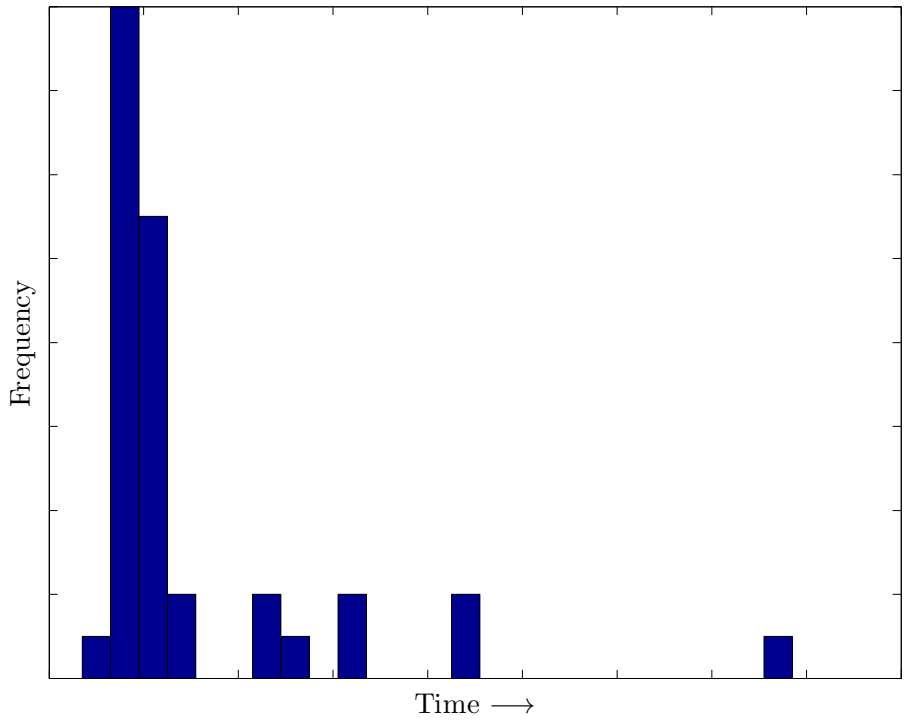

Figure 6.3: Distribution of duration from start index t_s to arrival at pull press threading from stoppage.

In Figure 6.4 is illustrated the distribution of duration from the web's arrival at the

pull press until the web has been taken to full width. The distribution of time taken to widen the web is relatively large. This may be be contributed to differences in how the shifts control the position of the web inside the pulp dryer.

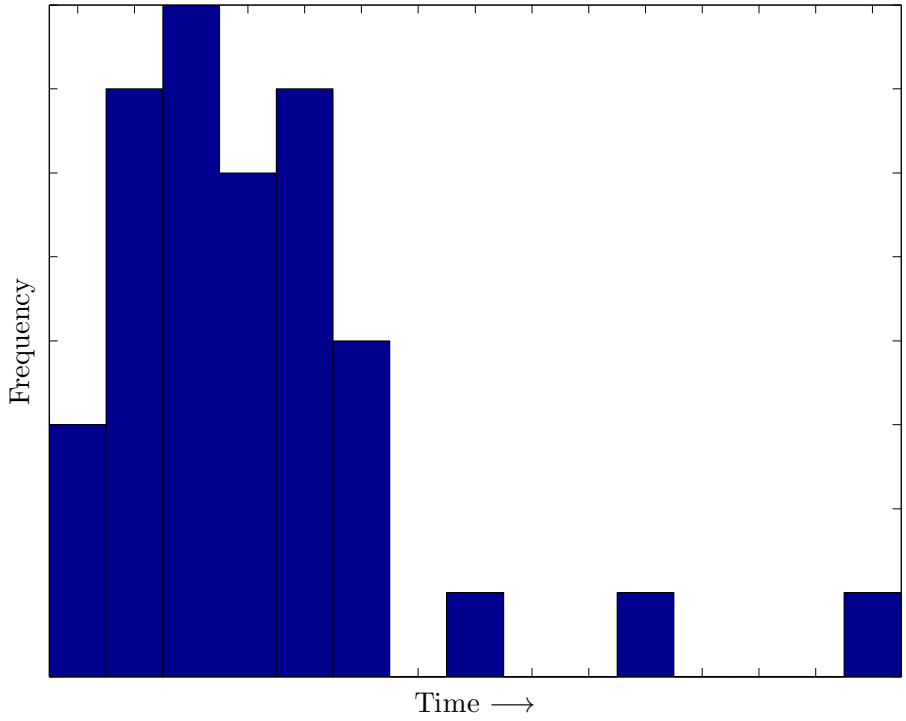

Figure 6.4: Distribution of duration from arrival at pull press to full width threading from stoppage.

After the web has been taken to full width, the quality of the pulp must is adjusted to meet the standards of the production plant. These include such parameters as correct weight and moisture content. Duration for this process stage is mainly low, but on some occasions this stage has taken a very long time in relation to average duration. The duration distribution for time taken from fully wide web until the closing of the recycling hatch and production is presented in Figure 6.5.

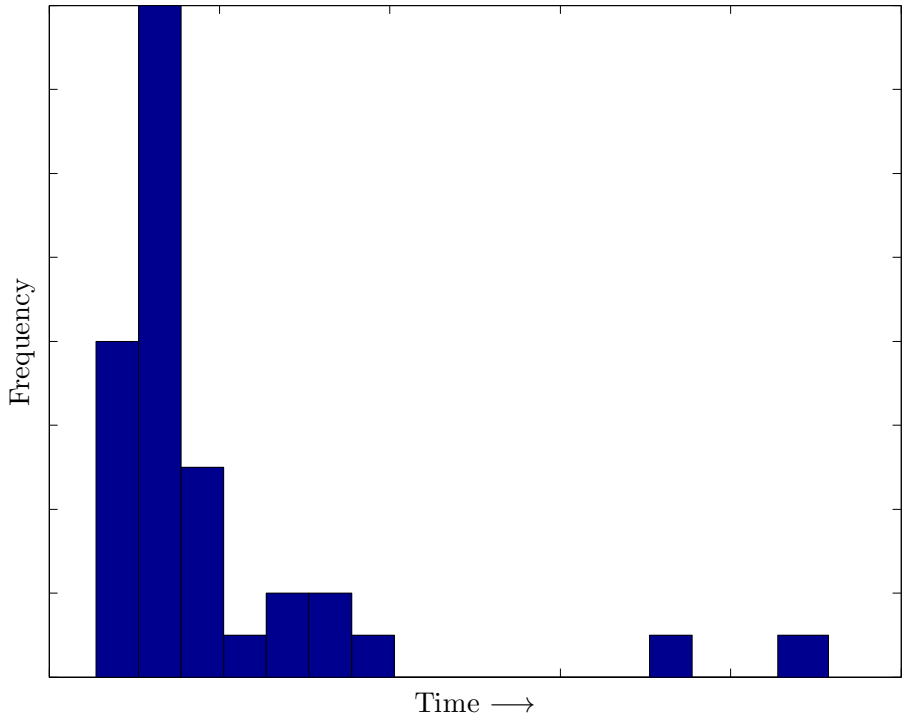

Figure 6.5: Distribution of duration from full width to production threading from stoppage.

There has been speculation at the plant that pieces of the narrow pulp web may be left inside the dryer even though the dryer is examined and cleaned after each unsuccessful threading attempt. However, the dryer may not be examined between threading efforts, i.e. while the threading tape is being turned and the air blowers turned on. As the web breaks between threading efforts, the narrow tail is suspected to leave pieces of pulp inside the dryer, and the following threading efforts to fail when the web collides with these pieces of pulp.

As discussed earlier, a threading attempt is defined in this thesis as a single turning instance for the threading tape, and may contain one or more threading efforts. A threading effort is defined to begin at the moment the web is at proper width for threading. In HMM's point of view, this corresponds to S_3^W. Figure 6.6 illustrates the average number of threading efforts, or the number of times the wet end state has changed to S_3^W, per threading attempts for each work shift. In the analysis, the data is limited similarly as in Figure 6.2, that is, the shift which begins the threading must also be the one ending it, either in web break, or success.

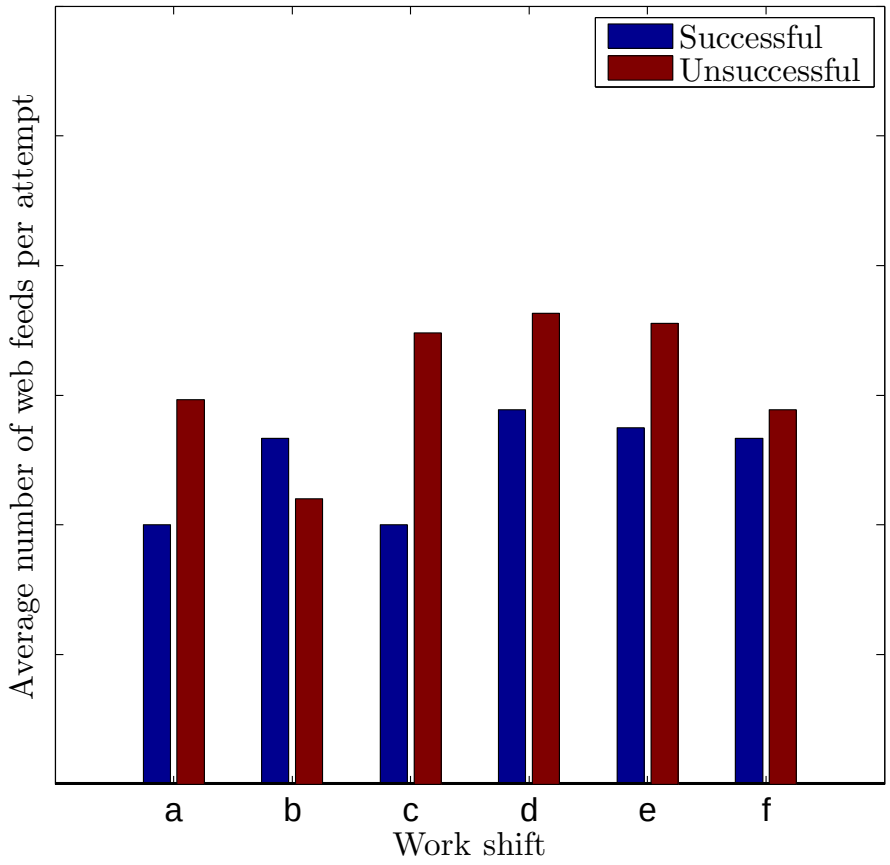

Figure 6.6: Average number of efforts per attempt for each shift threading from stoppage.

It should be noted, that the amount of data available for shift b is somewhat smaller compared to other shifts. Figure 6.6 shows how shifts a and c have the least number of web feeds per successful threading attempt on average compared to other shifts. For shift b the number of threading efforts per successful threading is larger than the average number of efforts on unsuccessful threadings. The situation is quite the opposite with all the other shifts. With shifts a and c through f, with an unsuccessful threading, the number of web feeds are larger compared to successful threadings.

In Figure 6.7 is presented the web break distribution between five of the main threading stages. Here, the percentage is the number of web breaks at the particular stage as opposed to the total number of web breaks for that shift. The stages numbered here 1 through 5 refer to web break from web feeding width, after the slack has been started to remove, the web having been lifted to the laser measurement, the web having been arrived at the pull press and the web being at full width.

Another way to consider these stages is that stage 1 the web has been at threading width, but for some reason the position of the web cutter is altered without the slack being removed. This may happen if the tail taken after the press section

breaks between the tape.

At stage 2 the slack is being removed, but the web does not arrive at the laser measurement.

At stage 3 the tail is taken through the airborne pulp dryer by the threading tape. At this point the shift workers must make changes to the dilution profile and altering the speed of the axial fans as discussed in Section 3.3.

Stage 4 refers to the phase of the threading procedure, where the narrow web has arrived at the pull press, and the web must be taken to full width. At this point the workers have the same methods of controlling the web as in the previous stage, but now the guide roll may also be used.

At stage 5 the web is at full width and is being prepared for cutting and baling. At this point only a few of the threading procedures lead to web break.

Figure 6.7 illustrates the distribution of web breaks for each work shift between these threading stages, as the threading is started from stoppage.

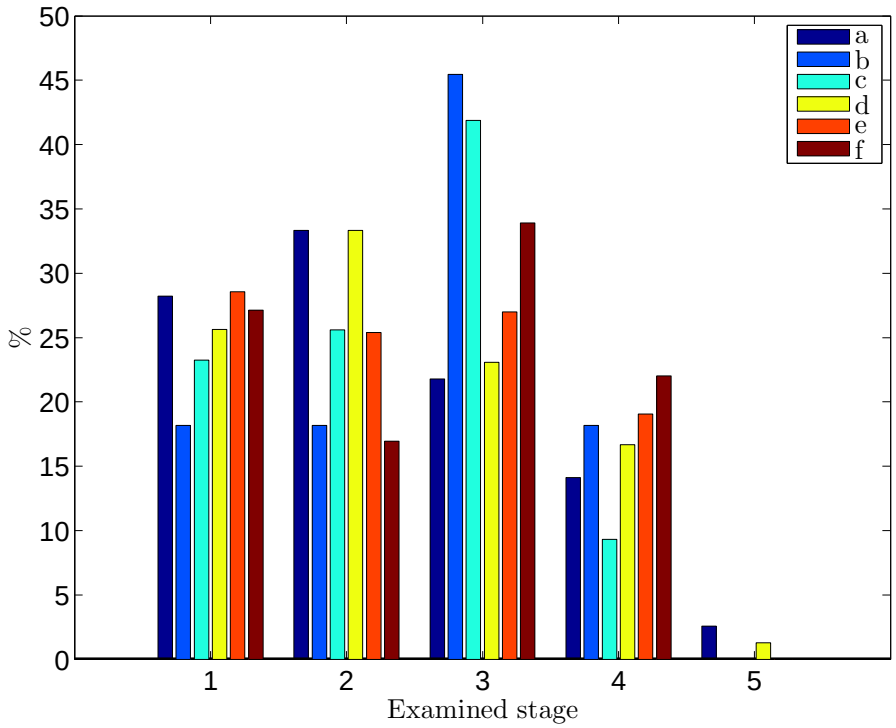

Figure 6.7: Web break distribution by state during threading from stoppage.

Figure 6.7 how for each work shift some of the work stages prove to be more difficult than others. For example for shifts b, c and f most of their web breaks occur when the tail is taken through the dryer.

6.2.2 Threadings from web break

In this section the characteristics are discussed as the threading procedure has begun from the web having been broken, as opposed to the plant having been in stoppage.

In Figure 6.8 the percentage for successful threadings from web break are presented. Compared to Figure 6.2 there are distinct similarities, with shift b having the highest percentage, followed by shifts d, e and f. However, the overall success rates are higher than in the case of threadings from stoppage.

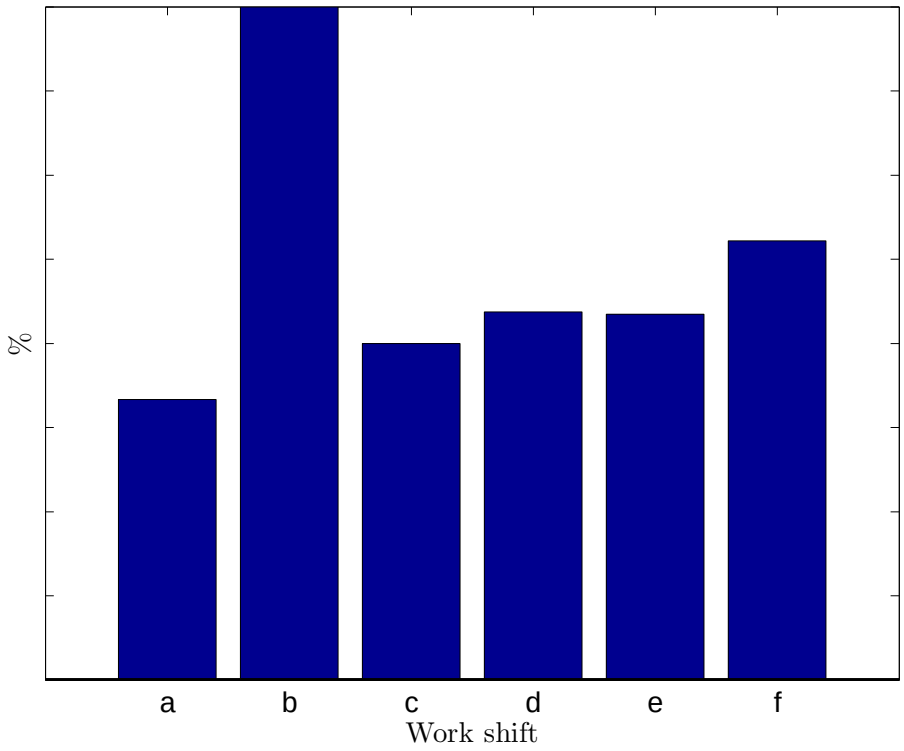

Figure 6.8: Percentage of successful threading attempts in relation to the shift's total number of threadings from break.

Figures 6.9 through 6.11 illustrate the duration distribution from one stage of the process to the next as in the case of threading starting from stoppage. It may be noted that the distributions are very alike compared to threadings from stoppage. The duration from start index to arrival at pull press is mainly low, with only individual threadings at which the process stage has taken longer. Again, the duration for the widening stage is is widely distributed.

The majority of threadings arrive at the pull press quickly. It may be noted, that the maximum frequency in Figures 6.9 and 6.3 is not at the shortest time interval. This is a result of the shifts' actions after the threading tape has been started. The web must be for example fed between the tape several times.

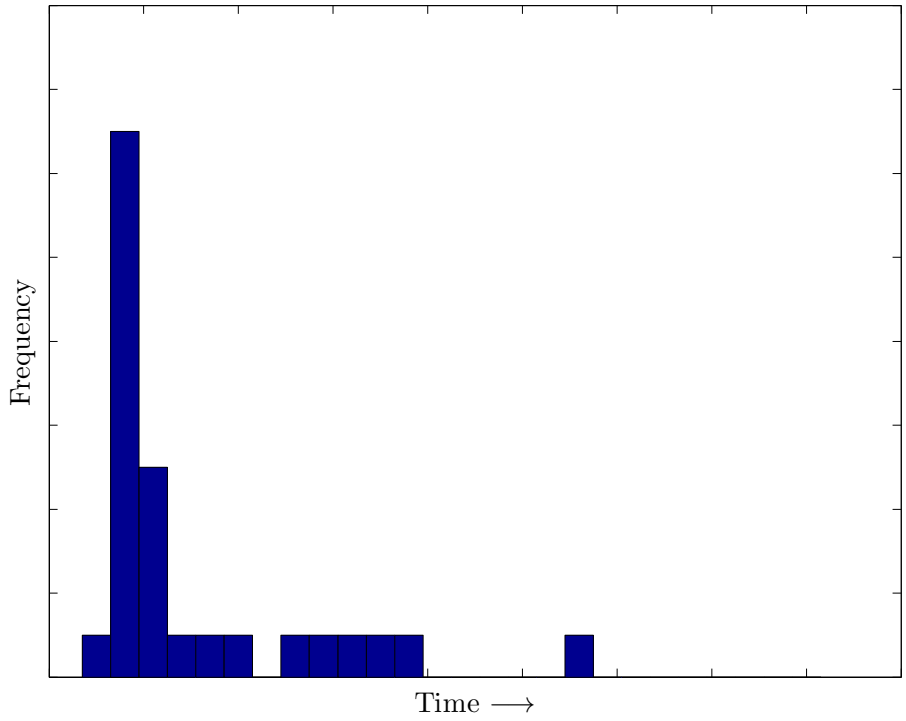

Figure 6.9: Distribution of duration from start index t_s to arrival at pull press threading from break.

The duration distribution from the tail's arrival at the pull press to the web being at full width threading from break is presented in Figure 6.10. The used axis are identical to those in Figure 6.4.

The widest distribution of duration in both threading from stoppage and break may be noticed from the arrival at the pull press to full width in Figure 6.4 for threadings from stoppage and 6.10 from break. This is affected by how often a shift changes the position of the web cutter and how large those changes are. As discussed earlier, the edge of the web may not be right next to the threading tape at the time of moving the cutter.

Figure 6.12 illustrates the average number of web feeds per threading attempt for each work shift. Here, for shift b there are no web feeds leading to unsuccessful threading, showing that every threading attempt they have made from web break have been successful.

The durations from full width to closing of the recycling hatch are presented in Figure 6.12. Again, very similarly to threadings from stoppage, the distribution is quite narrow. In the case of threadings from break, there are no out outliers as in the case of Figure 6.6.

Comparing the number of threading efforts per attempt, the overall number of efforts

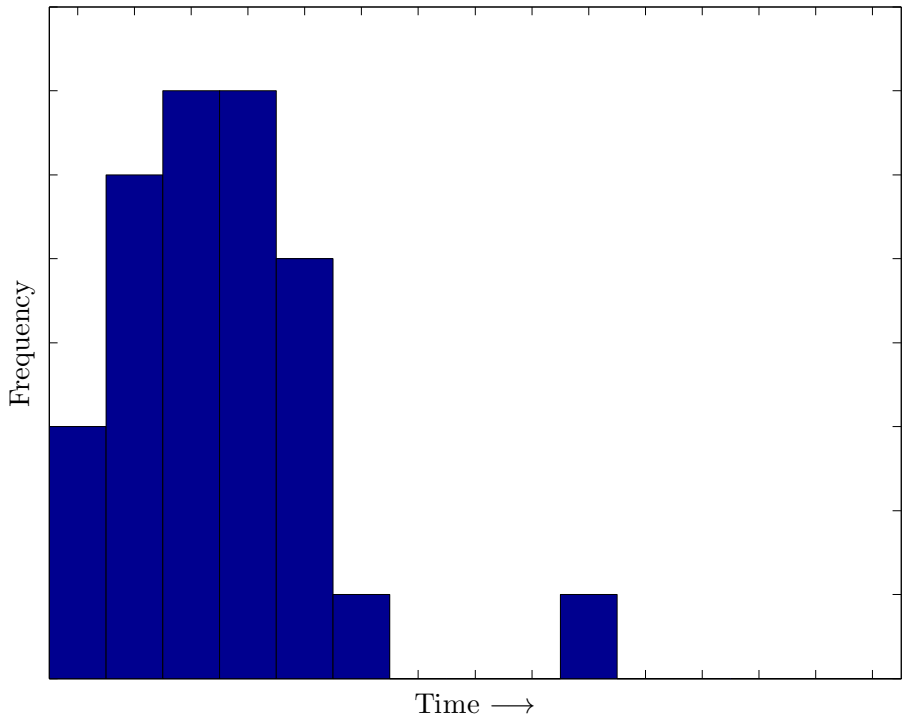

Figure 6.10: Distribution of duration from arrival at pull press to full width threading from break.

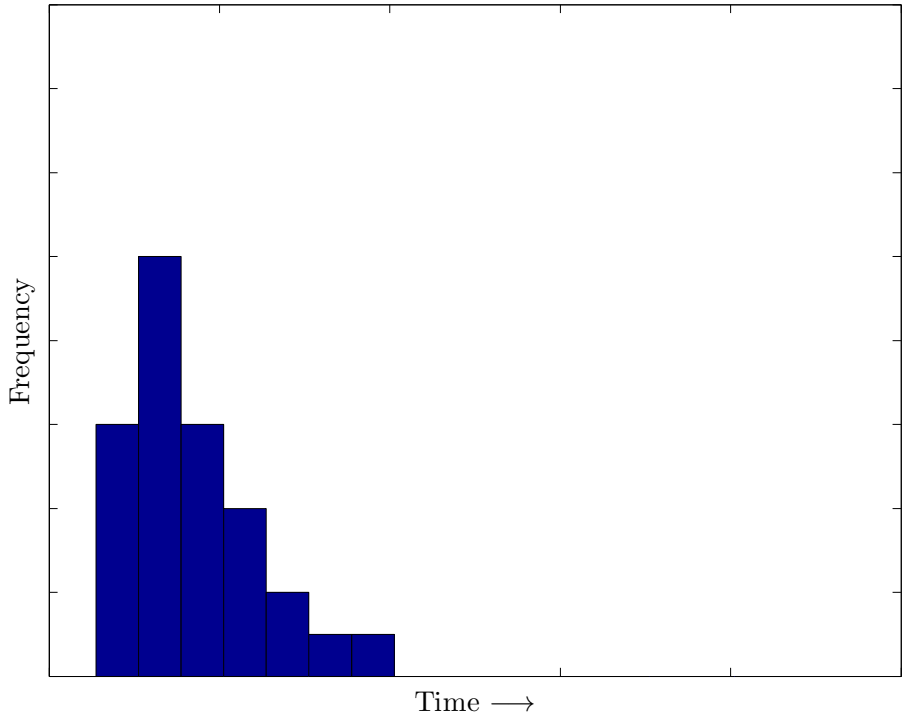

Figure 6.11: Distribution of duration from full width to production threading from break.

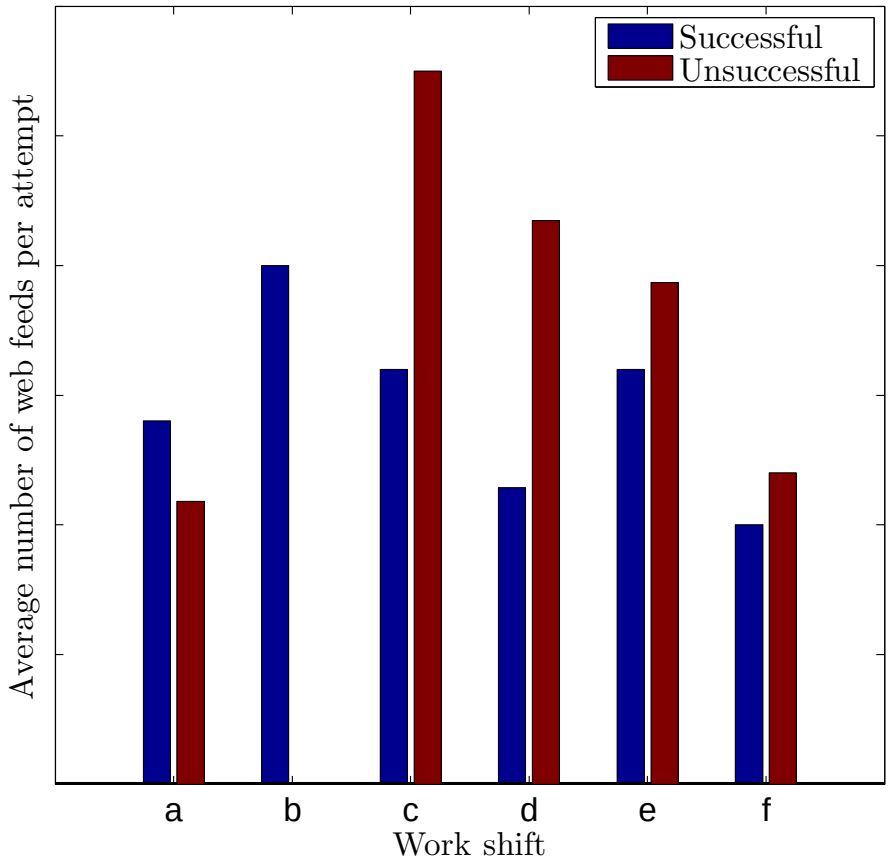

Figure 6.12: Average number of efforts per attempt for each shift threading from break.

is larger starting from web break. It may be noted that for shift c there are no unsuccessful threadings from web break. The number of web feeds is illustrated in Figure 6.12. From this illustration it may also be noted, that although the number of web feeds seems to correlate with the outcome of the threading, some shifts succeed even with higher number of attempts.

In Figure 6.13 the shifts' web break distributions for threadings starting from break is illustrated. Here it may be noted that the shifts have somewhat bigger differences in the distribution as opposed to the case of threading from stoppage, as in Figure 6.7. Also to be noted that although shift b had no unsuccessful threadings according to Figure 6.12, they still have a break distribution. This is due to the shift having more than one effort during the same attempt, which then result in successful threading. For the other shifts, the differences are much more noticeable than with the distributions between stages starting from stoppage. For example, shift a has very few web breaks at stage 1 as opposed to shift c. Also, shift c seems to have least problems as the tail is taken through the dryer at stage 3. Interestingly, the number of web breaks after the tail has arrived to the pull press, are significantly lower in threadings after a web break.

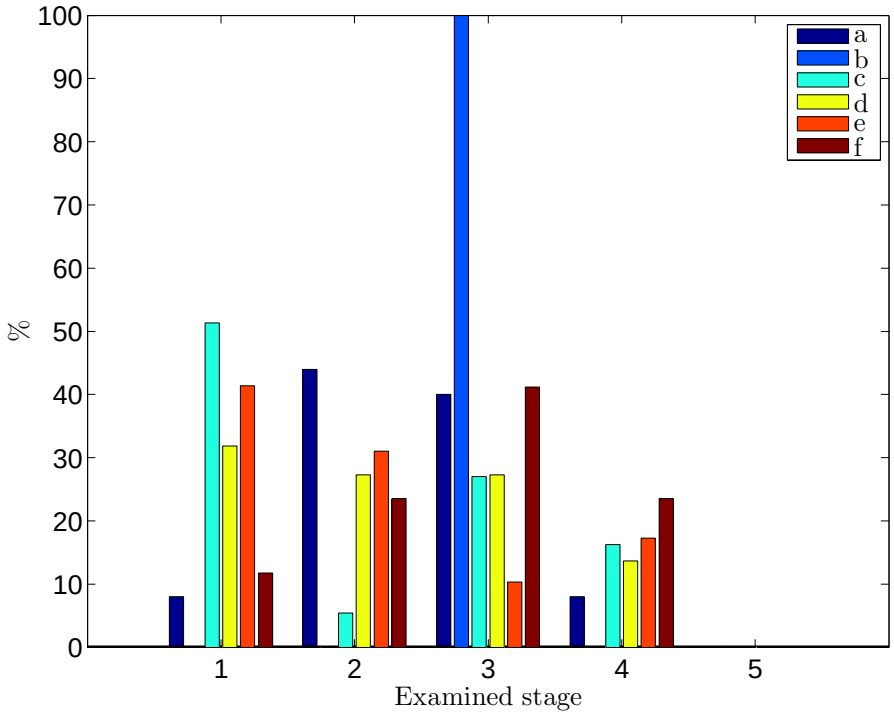

Figure 6.13: Web break distribution by state during threading from break.

6.3 Laser distance measurement issues

During the analysis of the Hidden Markov state vectors for the examined data, an issue with the laser distance measurement for the web between the press section and the pulp dryer occurred. On some occasions during the threading procedure, as the web has already been lifted to the laser measurement, the measurement suddenly rises to over 90%. Reason for this behaviour was not discovered during the research of this thesis.

As the measurement for the distance, that is to say, the web tension, has risen, the automation system attempts to counteract this by lowering the speeds for the machinery following the press section. This would under normal circumstances lower the web between the third press and the dryer. However, in the occurrences discovered, the distance measurement does not indicate the lowering of the web. An example for this behaviour is illustrated in Figure 6.14.

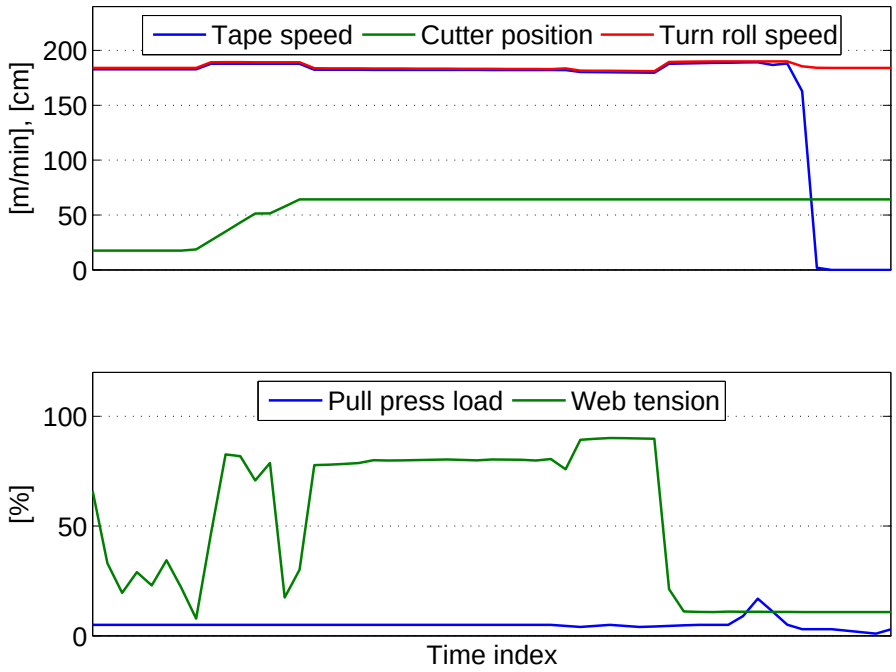

Figure 6.14: Example 1 of laser measurement behaviour during threading.

In Figure 6.14 it may be noticed, how the slack from the web is removed and the web is widened. The web is taken to the laser measurement, and the speed control is set to automated.

After some time, the tension measurement suddenly rises and the speeds for the tape and turn rolls are lowered. The web tension, however, is not affected by this. Suddenly the web tension measurement drops and the automation system tries to compensate this by accelerating the tape and turn rolls.

On another instance, the laser measurement is somewhat different. In Figure 6.15 the measurement rises to around 90%, and the web is taken to full width. At this point the web has been broken.

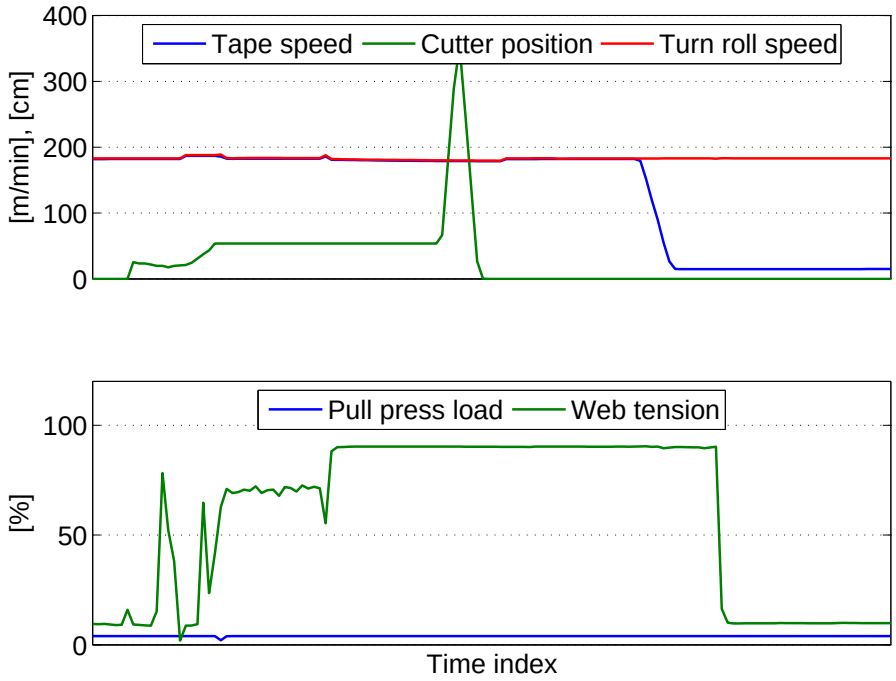

Figure 6.15: Example 2 of laser measurement behaviour during threading.

The laser measurement in Figure 6.15, however, measures the tension of the web as 90%, even after the tape has been stopped.

7. SUMMARY

In this thesis a tail threading procedure was examined and modelled using Hidden Markov Models. The pulp drying procedure and process environment were mainly studied through interviews with the staff at the plant.

The complex threading procedure was divided into separate tasks, and these tasks were defined as states for two Hidden Markov Models. Data of several threading attempts was collected from Stora Enso's database. Distinct features by which the different work stages could be recognized were extracted from the data. These features could, however, occur in several stages of the threading procedure, so in order to use them as observations for the HMM's, the features were combined using logical operators.

To avoid repetition in model definitions, the state sequence acquired from the dry end model was used to acquire observations for the wet end model. The parameters for each model were taught using supervised learning. The models were validated by comparing the true state sequence with the state sequence estimate determined by the HMM models. The results were calculated into confusion matrices. The confusion matrices suggested that the wet end model has more difficulty in determining the correct system state of the process. This may be contributed to the short duration of tasks in comparison with the low sampling rate available. Also, some inaccuracies in the process measurements give room for interpretation of the true system state. For the dry end model, over 99% confidence in state recognition was achieved.

State vectors were acquired for the gathered threading files using the developed models. From the state vectors, characteristics were calculated for further analysis. The characteristics included the duration of each tasks, the number of threading efforts. Also, in case the threading is unsuccessful, the work task during which the break occurs is acknowledged. The analysis of durations from web break and stoppage suggest that the shifts operate very similarly in both cases. The web break distribution analysis for threadings from stoppage suggests that the shifts have difficulties at same process stages. For threadings from web break, however, the shifts seem to have distinct strengths and limitations at different stages. This would suggest to further analyze the differences in the shifts' operation for best methods in each threading stage.

During the analysis of the HMM state sequences, some irregularities were discovered in the laser distance measurement between the press section and the airborne pulp dryer. The laser measurement would operate normally at the beginning of the threading procedure, but at some point the measurement begins to show higher values than normal. This causes the automation system to attempt to reduce the tension on the web by lowering the speed setpoints following the press section. The measurement, however, does not begin to decrease, and the threading ends in web break. Cause for the laser measurement behaviour was not found during the research of this thesis.

BIBLIOGRAPHY

[1] Andritz Fiber Drying AB. Fläkt drying systems for pulp & paper. http://atl.g.andritz.com/c/spectrum/00/00/61/6177/1/1/0/41935061/flaekt_dryer.pdf. accessed: 13.11.2012.

[2] L. E. Baum and T. Petrie. Statistical Inference and Probabilistic Functions of Finite State Markov Chains. *Annals of Math. Statistics*, 37, 1966.

[3] V. Bhusari and S. Patil. Study of hidden markov model in credit card fraudulent detection. *International Journal of Computer Applications*, 2011.

[4] Stora Enso. Stora Enso in Brief. http://www.storaenso.com/about-us/stora-enso-in-brief/Pages/stora-enso-in-brief.aspx. accessed: 31.10.2012.

[5] Pedro Fardim. *Chemical Pulping Part 1, Fibre Chemistry and Technology*, volume 6 of *Papermaking Science and Technology*. Paper Engineers' Association/Paperi ja puu Oy, Helsinki, Finland, 2011.

[6] Johan Gullichsen and Carl-Johan Fogelholm. *Chemical Pulping Part 2*, volume 6 of *Papermaking Science and Technology*. Fapet Oy, Helsinki, Finland, 2000.

[7] Johan Gullichsen and Carl-Johan Fogelholm. *Forest Products*, volume 3 of *Papermaking Science and Technology*. Fapet Oy, Helsinki, Finland, 2000.

[8] Fakhreddine O. Karray and Clarence de Silva. *Soft Computing and Intelligent Systems Design*. Pearson Education Limited, 2004.

[9] Metso. *Dryway Dryer Training Material*.

[10] Simo Nurmi. Selluradan leijutus ja hallinta ilmakuivaimessa. Master's thesis, Lappeenranta University of Technology, 2003.

[11] Lauri Palmroth. *Performance Monitoring and Operator Assistance Systems in Mobile Machines*. PhD thesis, Tampere University of Technology, 2011.

[12] Lawrence R. Rabiner. A Tutorial on Hidden Markov Models and Selected Applications in Speech Recognition. *Proceedings of the IEEE*, 77(22), 1989.

[13] Markku J. Seppälä, Ursula Klementti, Veli-Antti Kortelainen, Jorma Lyytikäinen, Heikki Siitonen, and Raimo Sironen. *Paperimassan valmistus*. Gummerus Kirjapaino Oy, 2001.

[14] Gary A. Smook. *Handbook for Pulp and Paper Technologists*. TAPPI, 1989.

[15] Sulzer. Pumping and mixing solutions for pulp and paper main processes. `http://www.sulzer.com/en/Industries/Pulp-and-Paper/Pumping-and-Mixing-Solutions-for-Pulp-and-Paper-Main-Processes`. accessed: 12.11.2012.

[16] Jan Sundholm. *Mechanical Pulping*, volume 5 of *Papermaking Science and Technology*. Fapet Oy, Helsinki, Finland, 1999.

[17] Kalevi Tervo. Human Adaptive Mechatronics Methods for Mobile Working Machines. Technical Report 168, Helsinki University of Technology, 2010.

[18] Suvi Vuorela. *Haastattelumenetelmät*. Tampere University, 2005.